# Possibility of superconductivity in the electron-hole liquid

G. Vignale* and K. S. Singwi
*Department of Physics and Astronomy, Northwestern University, Evanston, Illinois 60201*
(Received 30 August 1984)

It is shown that an electron-hole liquid under suitable conditions can become superconducting. This conclusion is reached by using an effective electron-electron interaction which includes vertex corrections and multiple electron-hole scattering by means of local-field corrections. A simple parametrization is proposed for the latter, and the parameters are determined in a self-consistent manner. The superconducting transition temperature $T_c$, the interaction parameters $\lambda$ and $\mu$, and the characteristic frequency $\omega_0$ are studied as functions of density, hole- to electron-mass ratio and valley degeneracy. $T_c$ is estimated to be of an observable magnitude ($T_c \sim 1$ K) in some cases of interest. The mechanism of superconductivity is purely based on Coulomb interactions. The intermediate bosons responsible for pairing of the electrons are *not* acoustic plasmons but correlated pair excitations from the Fermi sea of the holes.

## I. INTRODUCTION

Ever since its discovery, the electron-hole liquid[1] (EHL) in semiconductors has proved an ideal system to test various many-body theories of fermions interacting via a Coulomb potential. Agreement between theory and experiment has been very satisfactory. An interesting question to which, hitherto, no attention has been paid is, "can an electron-hole liquid become superconducting and, if so, under what conditions? Is the critical temperature sufficiently high to be observed in a laboratory experiment?" It is the purpose of this paper to examine these questions within the framework of existing many-body theories.

One of the simplest approaches to the problem is the one based on the random-phase approximation (RPA). In this approach the effective interaction between two electrons is assumed to be $v(q)/\epsilon(q,\omega)$, where $v(q)$ is the Fourier transform of the Coulomb potential and $\epsilon(q,\omega)$ is the RPA dielectric function of the system. An important feature of this interaction is the presence of an attractive term associated with acoustic plasmons,[2,3] a collective excitation which exists, in the RPA, whenever the ratio between the masses of the heavy and the light components exceeds 2.25. This suggests the possibility of a mechanism of superconductivity based on the exchange of acoustic plasmons.[4,5] The total RPA interaction is, however, always repulsive in the static limit. Superconductivity can therefore only arise as a result of the frequency dependence of the interaction, in particular, of the renormalization of the Coulomb repulsion parameter $\mu$. In the case of an EHL, with typical density $n \sim 10^{17}$–$10^{19}$ cm$^{-3}$, large background dielectric constant $\epsilon_\infty \sim 5$–$15$, effective masses of the order of the bare electron mass, and moderate hole-to electron-mass ratio $0.1 < \rho < 10$, an estimate of the superconducting transition temperature $T_c$ gives a vanishingly small value. This conclusion is erroneous because it is based on a theory, the RPA, which does not include many-body corrections to the effective interaction. One of the aims of this paper is to demonstrate the importance of such corrections. This demands a full reconsideration of the problem.

The two features that a realistic model of the interaction must necessarily include are (i) the existence of exchange and correlation between the particles of the system, and (ii) the existence of exchange and correlation between the two interacting particles and the rest of the system. In the language of Feynman diagrams, the first effect gives rise to vertex corrections to the *internal* polarization insertions and the second is responsible for vertex and ladder diagram corrections involving the *external* lines. A simple approximation scheme which enables us to treat both points (i) and (ii) in a unified way is the generalized random-phase approximation (GRPA). In this scheme exchange and correlation effects are described by certain local-field corrections which modify, at short range, the average Hartree field of the RPA. The local-field corrections can be calculated from a parameter-free theory, such as the one proposed some years ago by Singwi, Tosi, Land, and Sjölander[6] (STLS) and have been found to represent well the experimental data on the EHL.[7] Although the GRPA scheme was originally conceived to improve upon the RPA calculation of the dielectric function [i.e., to deal with point (i) only], we have found that it can be used to construct an effective, local interaction which consistently accounts for both effects (i) and (ii) by means of the local-field corrections. In its final form this effective interaction is very much like the two-component generalization of the one recently proposed by Kukkonen and Overhauser[8] for electrons in a simple metal. Different from the RPA interaction, it can be strongly attractive up to wave vectors of the order of the Fermi momentum and frequencies of the order of the Fermi energy of the holes (we assume that $m_h > m_e$). This behavior does not violate the conditions for the stability of the ground state with respect to spin- or charge-density waves. Thus, we can have a BCS-like situation, with Cooper pairs forming in an attractive potential well near the Fermi surface.

 

Using the GRPA form of the effective interaction, we have calculated the superconducting transition temperature of an EHL. We have assumed a simple parametrized form of the local fields which satisfies, in the limit of small wave vector, the appropriate compressibility sum rules. We have found that (1) $T_c$ is strongly dependent on the density of the liquid and decreases very rapidly when the latter increases, and (2) $T_c$ is strongly dependent on the mass ratio $\rho$ and decreases with the latter, falling to zero for $\rho < 3$. For the EHL in CdS,[9] a direct-band-gap semiconductor with one electron valley, one hole valley, and $\rho \sim 6$, we have estimated $T_c \sim 1$ K. For the EHL in AgBr,[10] an indirect-band-gap semiconductor with one electron valley, four equivalent hole valleys, and $\rho \sim 3$, we have estimated that $T_c \sim 0.1$ K. Thus, quite reasonable transition temperatures are possible, in principle, in an EHL, even with moderate values of the mass ratio. On the other hand, $T_c$ depends very sensitively on some parameters of the semiconductor, such as $\rho$, the reduced mass $\mu$, and the dielectric constant $\epsilon_\infty$, the last two determining the energy scale of the system. The choice of a suitable material becomes, therefore, a crucial factor for an experimental verification of our theory.

A few comments on the physical mechanism of superconductivity in the EHL are now in order. It is well known that exchange and correlation enhance the compressibility of a Fermi liquid, driving it toward a compressional instability which, in an EHL, would take place at $r_s = r_{sc} \cong 2.5$ ($r_s$ is the usual Coulomb coupling constant, measuring the average distance between carriers in units of the effective Bohr radius). Looking at the density fluctuation spectrum of the liquid, the progressive softening that occurs as $r_s$ approaches $r_{sc}$ shows as a constant shift of the spectral weight from high to low frequency. More precisely, in the limit of small $r_s$ (high-density limit) the spectral weight concentrates under the peak of the acoustic plasmon; as $r_s$ increases the acoustic-plasmon peak is gradually suppressed while the pair continuum is enhanced; as $r_s$ gets very near to $r_{sc}$, a new sharp peak appears on the low-frequency side, which we may call "paraphonon peak," and signals the proximity of a phase transition. In an EHL at equilibrium density, $r_s/r_{sc} \sim 0.8$ and the compressibility is enhanced by a factor of 4—5 relative to its noninteracting value. The situation is intermediate between the acoustic-plasmon regime ($r_s \to 0$) and the "paraphonon" regime ($r_s \to r_{sc}$), but somewhat nearer to the latter. The density-fluctuation spectrum consists of a continuous distribution of pair excitations from the Fermi sea of the holes whose density is enhanced by exchange and correlation effects. Whether these excitations can provide an effective mechanism for superconductivity depends very critically on the strength of their coupling to the electrons. It is here that exchange and correlation effects between the external particles and the medium play a decisive role. If they were neglected (i.e., if we used a simple screened interaction with a dielectric function accounting for internal exchange and correlation effects), the electron-hole effective potential would turn out to be rather weak. This effective potential, however, cannot be correct, since it fails to reduce, in the long-wavelength limit, to the inverse of the electronic density of states at the Fermi surface—a condition which was first pointed out by Heine, Nozières, and Wilkins (HNW).[11] Vertex corrections alone are sufficient to restore the HNW condition and to make the effective potential stronger than in the RPA. Electron-hole ladder diagrams add a further contribution in this direction by enhancing the probability for an electron and a hole to come near to each other. We can summarize the discussion by saying that the main attractive mechanism is the exchange of correlated pair excitations from the Fermi sea of the holes. There are many of them because the system is so compressible and they are strongly coupled to the electrons because of vertex corrections and electron-hole correlation. Thus, they can drive a superconducting transition.

In a recent paper, Jaffe and Achcroft[12] (JA) have investigated the interesting question of superconductivity in liquid metallic hydrogen (LMH). They arrive at the conclusion that LMH can become superconducting in a certain density range and that the transition temperature is around 100 K. The pairing mechanism, in their case, consists of the exchange of longitudinal phonons (acoustic plasmons) *and* pair excitation from the Fermi sea of the protons. The main difference between an EHL and LMH is in the value of the mass ratio, which is usually less than 10 in the former case and equal to $m_p/m_e \sim 1836$ in the latter. This difference has a number of important consequences. First, the mechanism based on exchange of acoustic plasmons is completely nonoperative in the EHL. Second, the transition temperature of an EHL is a very sensitive function of the mass ratio and its behavior is the opposite of what one would expect from an isotope-effect argument. Finally, it is precisely the smallness of the mass ratio that enables us to apply the GRPA scheme in which electrons and holes are treated on an equal basis and many-body corrections enter through local-field factors. It is interesting, in this respect, to compare the GRPA approach with the one taken by JA for liquid metallic hydrogen. In the JA method the central role is played by the so-called Elisahberg function $\alpha^2 F(\omega)$, which, in a crystalline solid, can be expressed in terms of the electron-ion pseudopotential and the spectral density of the phonons. In the case of liquid metallic hydrogen, JA identify these two quantities as the electron-proton effective interaction and the imaginary part of the density-density response function of the protons. The two quantities are determined independently in the JA scheme. For the first one they take the result of a density-functional calculation in LMH;[13] for the second they assume a GRPA-like form, adjusted to yield the correct compressibility of LMH. In our scheme, starting from the complete interaction between two electrons in the EHL, we can also separate the hole-mediated part of the interaction and use it to construct an Eliashberg function of the same form as JA. In our case, however, both the electron-hole interaction and the density-density response function of the holes are expressed in terms of a single set of local-field corrections. Even if these local fields are treated phenomenologically, they still must satisfy *three* independent constraints in the limit of small wave vector. Only one of these constraints can be associated with the compressibility sum

rule in its usual form. It would be very interesting to calculate the local-field corrections for LMH and compare the resulting $T_c$ with that of JA. Unfortunately, such a calculation is very difficult and, at present, intractable. The STLS theory, for example, stops converging for $\rho > 10$, while the phenomenological approach developed in this paper predicts too large an equilibrium density and binding energy for LMH. The difficulty is easy to understand if we recall that, because of their large mass, the protons in LMH have an effective coupling constant $r_s \sim 2000$. Thus, the GRPA scheme, which works very well for the EHL, cannot be easily extended to treat LMH.

This paper is organized as follows. In Sec. II we define the model and review the GRPA theory of the effective interaction. In Sec. III we propose a simple parametrization for the local-field corrections and calculate the parameters in a self-consistent manner. In Sec. IV we present results for the various interactions, the excitation spectra, and the parameters $\lambda$, $\mu$, and $\omega_0$. In Sec. V we calculate the critical temperature $T_c$ for various values of density, mass ratio, and valley degeneracy. In Sec. VI we present a critique of the calculation and discuss the possibility of experimental observation. In Appendix A we outline the derivation of the effective interaction. In Appendix B we formulate and discuss the conditions of stability of an EHL against spin- and charge-density waves. In Appendix C we give some details on the calculation of $T_c$.

## II. EFFECTIVE INTERACTION

The simplest model of an EHL consists of electrons and holes distributed in $\nu_1$ equivalent conduction bands with effective mass $m_e$ and $\nu_2$ equivalent valence bands with effective mass $m_h$, respectively. The carriers have an effective charge $\pm e/\epsilon_\infty^{1/2}$, where $\epsilon_\infty$ is the high-frequency dielectric constant of the semiconductor. The natural units of length and energy for this system are the excitonic Bohr radius $a_0^* = \hbar^2\epsilon_\infty/\mu e^2$ and the excitonic rydberg, $\mathrm{Ry}^* = e^2/2\epsilon_\infty a_0^*$, where $\mu^{-1} = m_e^{-1} + m_h^{-1}$ is the reduced mass. The model is thus completely specified by four parameters: the Coulomb coupling constant $r_s$ giving the average distance between two carriers in units of the excitonic Bohr radius [$n^{-1} = \frac{4}{3}\pi r_s^3 (a_0^*)^3$, where $n$ is the total density of electron-hole pairs], the mass ratio $\rho = m_h/m_e$, and the valley degeneracies $\nu_1$ and $\nu_2$. The absolute sign of the charge does not matter in this model, as long as there are two kinds of carriers with opposite charge. We shall always call "holes" the heavier particles, irrespective of their nature, and by this definition $\rho$ is always greater than 1.

We now introduce the density-density response matrix $\chi_{ij}^s(q,\omega)$, which describes the linear response of the EHL to external fields $V_1, V_2$ coupling to the total density of electrons and holes, respectively. The induced densities are

$$\delta n_i(q,\omega) = \sum_{j=1}^{2} \chi_{ij}^s(q,\omega) V_j(q,\omega), \quad i = 1,2 \ . \tag{1}$$

where we use the subscript 1 to denote electrons and the subscript 2 to denote holes. In the GRPA one assumes that the system responds as a noninteracting one to an effective field which is the superposition of external, Hartree, and exchange plus correlation fields:

$$\delta n_i(q,\omega) = \chi_{0i}(q,\omega) \left[ V_i(q,\omega) + \sum_{j=1}^{2} \psi_{ij}^s(q) \delta n_j(q,\omega) \right] , \tag{2}$$

where $\chi_{01(2)}$ is the polarizability of noninteracting electrons (holes) and

$$\psi_{ij}^s(q) = \Phi_{ij}(q)[1 - G_{ij}^s(q)] \tag{3}$$

are the spin-symmetric polarization fields in which

$$\Phi_{ij}(q) = \frac{4\pi e_i e_j}{\epsilon_\infty q^2} \tag{4}$$

is the Fourier transform of the Coulomb potential between particles $i$ and $j$. Here, the $G_{ij}^s(q)$ are the spin-symmetric local-field corrections which account for exchange and correlation effects between components $i$ and $j$. The designation of the "spin-symmetric" corrections derives from the fact that those local fields are averages over the possible spin orientations—as well as the band indices—of the two particles:

$$\begin{aligned} G_{ii}^s &= \frac{1}{\nu_i} \left[ \frac{G_{ii}^{\uparrow\uparrow,\mathrm{intra}} + G_{ii}^{\uparrow\downarrow,\mathrm{intra}}}{2} \right. \\ &\quad \left. + (\nu_i - 1) \frac{G_{ii}^{\uparrow\uparrow,\mathrm{inter}} + G_{ii}^{\uparrow\downarrow,\mathrm{inter}}}{2} \right] , \\ G_{ij}^s &= G_{ij}, \quad i \neq j \end{aligned} \tag{5}$$

where the superscripts $\uparrow\uparrow$ and $\uparrow\downarrow$ refer to the parallel and antiparallel spins situation and the superscripts "intra" (for *intra*valley) and "inter" (for *inter*valley) indicate that the two particles are in the same band or in different bands, respectively. The four local-field corrections $G^{\uparrow\uparrow,\mathrm{intra}}$, $G^{\uparrow\downarrow,\mathrm{intra}}$, $G^{\uparrow\uparrow,\mathrm{inter}}$, and $G^{\uparrow\downarrow,\mathrm{inter}}$ are, in principle, independent. In practice, however, one can neglect transitions in which a particle scatters from one band to another, since they require a momentum transfer of the order of 100 times the Fermi momentum. In this approximation there is no difference between $G^{\uparrow\downarrow,\mathrm{intra}}$, $G^{\uparrow\uparrow,\mathrm{inter}}$, and $G^{\uparrow\downarrow,\mathrm{inter}}$ (since, in all these cases, there is no exchange), and we can set $G^{\uparrow\downarrow,\mathrm{intra}} = G^{\uparrow\uparrow,\mathrm{inter}} = G^{\uparrow\downarrow,\mathrm{inter}} \equiv G^{\uparrow\downarrow}$ and $G^{\uparrow\uparrow,\mathrm{intra}} \equiv G^{\uparrow\uparrow}$. For $i \neq j$ there is, of course, no question of spin or band dependence of the local-field correction. Comparing Eqs. (1) and (2), we immediately find that

$$[(\underline{\chi}^s)^{-1}]_{ij}(q,\omega) = [\chi_{0i}(q,\omega)]^{-1}\delta_{ij} - \psi_{ij}^s(q) \ , \tag{6}$$

where $(\underline{\chi}^s)^{-1}$ is the inverse of the matrix $\underline{\chi}^s$. Approximations, which go under different names, to the response functions of Eq. (1) are, indeed, approximations for the local-field factors $G_{ij}^s$.

In a similar way, we introduce the spin-response matrix $\chi_{ij}^a(q,\omega)$, which describes the response of the EHL to external fields coupling to the spin density of electrons and holes, respectively. Neglecting magnetic interactions between electrons and holes, this matrix turns out to be diagonal and its GRPA expression is

$$\chi^a_{ij}(q,\omega)=\frac{\chi_{0i}(q,\omega)}{1-\psi^a_{ii}(q)\chi_{0i}(q,\omega)}\delta_{ij}\ , \tag{7}$$

where

$$\psi^a_{ii}(q)=-\Phi_{ii}(q)G^a_{ii}(q) \tag{8}$$

and

$$G^a_{ii}(q)=\frac{1}{\nu_i}\left[\frac{G^{\uparrow\uparrow,\text{intra}}_{ii}-G^{\uparrow\downarrow,\text{intra}}_{ii}}{2}+(\nu_i-1)\frac{G^{\uparrow\uparrow,\text{inter}}_{ii}-G^{\uparrow\downarrow,\text{inter}}_{ii}}{2}\right]$$

$$\cong\frac{G^{\uparrow\uparrow}_{ii}-G^{\uparrow\downarrow}_{ii}}{2\nu_i} \tag{9}$$

are the spin-antisymmetric local-field factors. The local-field factors will play a major role in the rest of this paper. They can be calculated, in principle, from the self-consistent scheme of Singwi *et al.*[6] with the modifications needed to satisfy the compressibility and susceptibility sum rules. In the small-$q$ limit they vanish as $q^2$, removing the singularity in $\Phi_{ij}$, and in the large-$q$ limit they tend to a constant value related to the pair correlation function at zero separation.

Let us now introduce the effective interaction between two electrons in the EHL. In another paper[14] we discuss in detail how to use the local-field factors to construct an effective interaction which consistently includes exchange and correlation within the medium and with the medium. The interested reader will find a condensed but complete description of our method in Appendix A of the present paper. The final result for the effective interaction between two electrons in the singlet state is

$$V_{\text{eff}}(q,\omega)=v(q)+\sum_{i,j=1}^{2}\psi^s_{1i}(q)\chi^s_{ij}(q,\omega)\psi^s_{j1}(q)-(2\nu_1+1)[\psi^a_{11}(q)]^2\chi^a_{11}(q,\omega)\ , \tag{10}$$

where $v(q)=\Phi_{11}(q)$. This expression differs from the normally used dielectric interaction

$$v(q)/\epsilon(q,\omega)=v(q)+\sum_{i,j=1}^{2}\Phi_{1i}(q)\chi^s_{ij}(q,\omega)\Phi_{j1}(q) \tag{11}$$

in two respects. First, the effective potential by which the interacting electrons polarize the medium and "feel" the polarization of the medium is not the bare Coulomb potential $\Phi_{ij}(q)$ but rather the polarization potential $\psi^s_{ij}(q)$. This difference reflects the fact that the dielectric form of the interaction treats the interacting electrons as test particles, whereas ours treats them on the same basis as the other electrons of the system. Second, Eq. (10) has an extra term which describes an interaction *via* spin fluctuations of the electron subsystem. This term is multiplied by a factor $(2\nu_1+1)$, 1 for longitudinal spin fluctuations and $2\nu_1$ for transverse spin fluctuations. Apart from the precise identification of the local-field factors entering it, Eq. (10) is the two-component, frequency-dependent generalization of the effective interaction proposed by Kukkonen and Overhauser[8] for electrons in a simple metal.

Equation (10) can be written in a different form that is more convenient for the calculation of the superconducting parameters. We isolate that part of the interaction which is mediated by the holes. Using the GRPA expressions for $\chi^s$ and $\chi^a$, after a certain amount of algebra we find

$$V_{\text{eff}}(q,\omega)=U_c(q,\omega)+U_h(q,\omega)\ , \tag{12a}$$

where

$$U_c=\frac{\Lambda_1^2 v}{\epsilon_1}+(vG^s_{11})^2\frac{\chi_{01}}{1+vG^s_{11}\chi_{01}}-(2\nu_1+1)(vG^a_{11})^2\frac{\chi_{01}}{1+vG^a_{11}\chi_{01}} \tag{12b}$$

and

$$U_h=v^2_{eh}\chi^s_{22}\ . \tag{12c}$$

In writing these formulas we have introduced the proper vertex function of the electrons,

$$\Lambda_1=1/(1+v\chi_{01}G^s_{11})\ , \tag{13a}$$

the electronic dielectric function,

$$\epsilon_1=1-v\chi_{01}\Lambda_1\ , \tag{13b}$$

the electron-hole effective potential,

$$v_{eh}=\frac{\psi_{12}}{1-\psi^s_{11}\chi_{01}}=\frac{\psi_{12}\Lambda_1}{\epsilon_1}\ , \tag{13c}$$

the hole-hole component of the density-density response function,

$$\chi^s_{22}=\frac{\chi_{02}}{1-f\chi_{02}}\ , \tag{13d}$$

and the hole-hole interaction function,

$$f=\psi^s_{22}+(\psi^s_{12})^2\frac{\chi_{01}}{1-\psi^s_{11}\chi_{01}}\ . \tag{13e}$$

In all these formulas the dependence on $q$ and $\omega$ is understood.

A few comments are now in order to explain the physical meaning of the various terms in this apparently complicated expression. The first term on the right-hand side of Eq. (12a) represents the interaction between two electrons in the absence of holes. From Eq. (12b) we see that there are three contributions to it. The first one is the Coulomb interaction screened by electronic polarization and multiplied by the square of the frequency-dependent vertex correction [Eq. (13a)]. This form of the vertex correction was first used, in the static limit, by Kukkonen and Wilkins[15] (KW) in a calculation of thermal resistivity of the electron gas. It satisfies the Ward identities[16] in the limit of small $q$ and $\omega$, if $G^s_{11}$ is chosen to satisfy the compressibility sum rule and if mass renormalization is

neglected. The second and third terms of Eq. (12b) represent the contribution of ladder diagrams in the particle-hole channel. The second is associated with density fluctuations and tends to reduce the repulsion between two electrons. The third is associated with spin-density fluctuations, both longitudinal and transverse, and increases the repulsion between two electrons in the singlet state. Equation (12c) gives the hole-mediated part of the interaction. It has the same structure as the phonon-mediated interaction in a metal, i.e., the square of an electron-phonon matrix element times the phonon propagator. The electron-hole effective potential, given in Eq. (13c), is a screened, vertex-corrected Coulomb interaction. Note that, while the screening is purely electronic, the vertex correction is due to both electrons (the factor $\Lambda_1$) and holes (the factor $1-G_{12}$ in $\psi_{12}$). This last correction—which is the analog of a phonon correction to the electron-phonon vertex—can be quite large at finite wave vectors for the values of the mass ratio under consideration. This is like saying that Migdal's theorem does not apply to an EHL. In the small-$q$ limit the electron-hole potential should reduce to the HNW limit,[11]

$$\lim_{q\to 0} |v_{eh}(q)| = 1/[2N_1(0)] , \tag{14}$$

where $N_1(0)$ is the electronic density of states per spin at the Fermi surface. Our expression for $v_{eh}(q)$ satisfies this condition.

With Eqs. (12) and (13) we have the basis tool for investigating the possibility of superconductivity in an EHL. The rest of this paper is just a closer examination of the physics contained in Eqs. (12).

## III. LOCAL-FIELD CORRECTIONS

In this section we shall give quantitative expressions for the local-field corrections to be used in the calculations of the effective interaction. A first-principles approach, such as STLS, would lead to a cumbersome numerical problem, if one wants to satisfy the three compressibility sum rules for the three spin-symmetric $G$'s. Such a calculation is beyond the scope of the present paper and is, in fact, not warranted at this stage. We choose, instead, a phenomenological approach similar to the one recently proposed by Pines *et al.*[17] for the electron liquid. The idea is to parametrize the local-field factors by a simple Hubbard-like form which satisfies the sum rules in the small-$q$ limit and reduces to the STLS limit for large $q$.

Let us first consider the small-$q$ limit of the spin-symmetric local fields. Suppose we change independently the densities of electrons and holes in the volume by small amounts $\delta n_1$ and $\delta n_2$. In order to do this we imagine the transfer of electrons and holes from an external reservoir of particles to the volume under consideration. The total work needed for this transformation (i.e., the variation of internal energy plus the work necessary to transfer the additional particles from the reservoir to this system) is, per unit volume,

$$\delta W = \frac{1}{2}\frac{\partial^2\epsilon_v}{\partial n_1^2}\bigg|_{n_1=n_2=n}\delta n_1^2 + \frac{1}{2}\frac{\partial^2\epsilon_v}{\partial n_2^2}\bigg|_{n_1=n_2=n}\delta n_2^2 + \frac{\partial^2\epsilon_v}{\partial n_1\,\partial n_2}\bigg|_{n_1=n_2=n}\delta n_1\,\delta n_2 + \tfrac{1}{2}\lim_{q\to 0}[v(q)(\delta n_2-\delta n_1)^2] , \tag{15}$$

where $\epsilon_v(n_1,n_2)$ is the energy per unit volume of a homogeneous EHL in which the net charge density $n_2-n_1$ is compensated by a rigid background of charge. The Coulomb energy introduced by breaking charge neutrality is explicitly accounted for by the last term of Eq. (15). The necessary work $\delta W$ can also be computed by taking the small-$q$ limit of the Hohenberg-Kohn expansion[18] for the energy of a slightly inhomogeneous EHL. This expansion reads

$$\epsilon_v(n+\delta n_1(\mathbf{r}), n+\delta n_2(\mathbf{r})) - \epsilon_v(n) = -\tfrac{1}{2}\sum_{\mathbf{q}}\sum_{i,j=1}^{2}\delta n_i(-\mathbf{q})[(\chi^s)^{-1}]_{ij}(q,0)\delta n_j(\mathbf{q}) , \tag{16}$$

where $\epsilon_v(n)$ is the energy per unit volume of the homogeneous ground state with equal densities of electrons and holes, and the $\delta n_i(\mathbf{q})$ are the Fourier transforms of the infinitesimal density modulations $\delta n_i(\mathbf{r})$. Equating the right-hand sides of Eqs. (15) and (16), the latter in the small-$q$ limit, and using the GRPA expression for $(\chi^s)^{-1}$ [Eq. (6)], we find

$$\lim_{q\to 0}[\psi^s_{ij}(q) - \chi_{0i}^{-1}(q,0)] = \frac{\partial^2\epsilon_v(n_1,n_2)}{\partial n_i\partial n_j}\bigg|_{n_1=n_2=n} + \lim_{q\to 0}[\phi_{ij}(q)] . \tag{17a}$$

Repeating the argument for a noninteracting EHL, we find

$$-\lim_{q\to 0}[\chi_{0i}^{-1}(q,0)] = \frac{\partial^2\epsilon_{0v}(n_1,n_2)}{\partial n_i^2}\bigg|_{n_1=n_2=n} , \tag{17b}$$

where $\epsilon_{0v}$ is the kinetic energy per unit volume of the noninteracting EHL. We define the exchange-correlation energy per unit volume as

$$\epsilon_{v\,\mathrm{xc}}(n_1,n_2) \equiv \epsilon_v(n_1,n_2) - \epsilon_{0v}(n_1,n_2) . \tag{18}$$

Subtracting Eq. (17b) from (17a) and using the definitions of $\psi^s_{ij}$ [Eq. (3)], we finally find

$$\lim_{q\to 0}[\Phi_{ij}(q)G^s_{ij}(q)] = -\frac{\partial^2\epsilon_{v\,\mathrm{xc}}(n_1,n_2)}{\partial n_i\,\partial n_j}\bigg|_{n_1=n_2=n} . \tag{19}$$

This set of equations represents the two-component generalization of the well-known compressibility sum rule. The compressibility itself is given by a suitable combination of the second derivatives of the energy:

$$\kappa^{-1}=n^2\frac{d^2\epsilon_v(n,n)}{dn^2}$$
$$=\kappa_f^{-1}+n^2\frac{d^2\epsilon_{v\,\mathrm{xc}}(n,n)}{dn^2}$$
$$=\kappa_f^{-1}+n^2\left[\frac{\partial^2\epsilon_{v\,\mathrm{xc}}}{\partial n_1^2}+\frac{\partial^2\epsilon_{v\,\mathrm{xc}}}{\partial n_2^2}+2\frac{\partial^2\epsilon_{v\,\mathrm{xc}}}{\partial n_1\,\partial n_2}\right]_{n_1=n_2=n}, \tag{20}$$

where

$$\kappa_f^{-1}=\tfrac{2}{3}n(E_{Fe}+E_{Fh}) \tag{21}$$

is the inverse of the noninteracting compressibility and $E_{Fe}$ ($E_{Fh}$) is the Fermi energy of the electrons (holes). Using Eqs. (19)—(21) it is easy to derive the important result

$$\frac{\kappa_f}{\kappa}=1-2\gamma\lim_{q\to 0}\left[\frac{G_{11}^s(q)+G_{22}^s(q)-2G_{12}(q)}{(q/q_F)^2}\right], \tag{22a}$$

which gives the compressibility ratio in terms of the small-$q$ limit of the local-field factors. Here we have introduced the notation

$$\frac{1}{\gamma}=\frac{1}{\gamma_1}+\frac{1}{\gamma_2},\quad \gamma_i=\frac{2\alpha r_s}{\pi}\frac{m_i}{\mu}\nu_i^{2/3}, \tag{22b}$$

where $\alpha=(4/9\pi)^{1/3}$ and $q_F=(3\pi^2 n)^{1/3}$. This ratio vanishes when the compressional instability is reached. Notice that, since $G_{12}<0$, $\kappa_f/\kappa$ is always less than 1.

In order to calculate the second derivatives in Eq. (19), it is convenient to introduce a dimensionless exchange-correlation energy per electron (hole), $\epsilon_{\mathrm{xc}}^{(i)}(r_{si},x)$ [$i$ denotes electron (hole)], in which $r_{si}$ refers to the electron (hole) density and $x$ is the hole-to electron-density (electron-to hole-density) ratio. More precisely,

$$\epsilon_{v\,\mathrm{xc}}(n_1,n_2)\equiv n_1\epsilon_{\mathrm{xc}}^{(1)}(r_{s_1},n_2/n_1)\,\mathrm{Ry}^*$$
$$\equiv n_2\epsilon_{\mathrm{xc}}^{(2)}(r_{s_2},n_1/n_2)\,\mathrm{Ry}^*\ . \tag{23}$$

Using this definition in Eq. (19), we find, after some simple algebra,

$$g_{ii}^s\equiv\lim_{q\to 0}\left[\frac{G_{ii}^s(q)}{(q/q_F)^2}\right]=-\frac{r_s}{6\alpha^2}\left.\frac{\partial^2\epsilon_{\mathrm{xc}}^{(i)}(r_s,x)}{\partial x^2}\right|_{x=1}. \tag{24}$$

The small-$q$ limit of $G_{12}(q)$ is most easily calculated from Eq. (22). Using the second part of Eq. (20) and Eq. (21), together with the relation $n\,d/dn=-\frac{1}{3}r_s\,d/dr_s$, we find

$$\frac{\kappa_f}{\kappa}-1=\frac{\alpha^2 r_s^3}{6}\left[r_s\frac{d^2\epsilon_{\mathrm{xc}}(r_s)}{dr_s^2}-2\frac{d\epsilon_{\mathrm{xc}}(r_s)}{dr_s}\right]\frac{\tilde{\mu}}{\mu}, \tag{25}$$

where $\epsilon_{\mathrm{xc}}(r_s)\equiv\epsilon_{\mathrm{xc}}^{(i)}(r_s,x=1)$ is the dimensionless exchange-correlation energy per particle for equal densities of electrons and holes, and $\tilde{\mu}$ is the reduced mass corresponding to the effective masses $m_1\nu_1^{2/3}$ and $m_2\nu_2^{2/3}$. Using Eq. (22), we find

$$g_{12}\equiv\lim_{q\to 0}\left[\frac{G_{12}(q)}{(q/q_F)^2}\right]=\frac{g_{11}^s+g_{22}^s}{2}+\frac{1}{4\gamma}\left[\frac{\kappa_f}{\kappa}-1\right]. \tag{26}$$

Having fixed the small-$q$ limit of the local fields, we recall that, within the STLS theory,

$$\lim_{q\to\infty}[G_{ij}^s(q)]=1-C_{ij}^0\ , \tag{27}$$

where $C_{ij}^0$ is the $i$-$j$ pair correlation function at zero separation. The simplest form that smoothly interpolates between the limits of Eqs. (24)—(27) is the Hubbard-like form,

$$G_{ij}^s(q)=\frac{g_{ij}^s(1-C_{ij}^0)q^2}{(1-C_{ij}^0)+g_{ij}^s q^2}\ , \tag{28}$$

and this is the one that we are going to use in our calculations. The pair correlation parameters $C_{ij}^0$ can be taken from the results of previous workers.[7,19] In particular, $C_{11}^0$ and $C_{22}^0$ turn out to be quite small at the densities of interest, $C_{ii}^0\le 0.1$, and can be safely set equal to zero in Eq. (27). The $r_s$ dependence of the electron-hole enhancement factor $C_{12}^0$ has been calculated by Vashishta *et al.*[7] and is given in Table I. This quantity is comparable to or larger than unity and increases sharply when $r_s$ increases. Recent measurements[20] of the electron-hole recombination time in an EHL in Ge are in excellent quantitative agreement with this theory. On the other hand, the mass dependence of $C_{eh}^0$ turns out to be very slight, as can be seen from the calculations of Chakraborty *et al.*[19] Up to $\rho=50$ it can be accurately fitted by the formula

$$1-C_{12}^0(\rho)=\frac{1-C_{12}^0(\rho=1)}{1+0.0156(\rho-1)^{1/2}}\ . \tag{29}$$

We said at the end of Sec. II that the local-field correction $G_{12}(q)$ in the electron-hole potential is analogous to a phonon vertex correction to the electron-phonon matrix element. In the limit of very large $\rho$ this correction decreases as $\rho^{-1/2}$, a result somewhat reminiscent of Migdal's theorem.

The "thermodynamic" parameters $g_{ij}$ can be determined self-consistently as follows. We start with an initial guess for $g_{ij}$'s and use Eq. (28) with the known values of the $C_{ij}^0$'s to calculate the response functions $\chi_{ij}^s$ given in Eq. (5). The densities of the two components are taken to be $n_1=n$ and $n_2=nx$ in the calculation of $\epsilon_{\mathrm{xc}}^{(1)}(r_s,x)$, and $n_1=nx$ and $n_2=n$ in the calculation of $\epsilon_{\mathrm{xc}}^{(2)}(r_s,x)$. We recall that the Lindhard functions for the imaginary frequency $i\omega$ are given by

TABLE I. Parameters of the spin-symmetric local-field corrections: $g_{ij}^s$ from Eqs. (24)—(26), $g$ from Eq. (37), and $c_{12}^0$ from Eq. (27).

| | $\nu_1=\nu_2=1$, $\rho=6$ | | | | |
|---|---|---|---|---|---|
| $r_s$ | $g_{11}^s$ | $g_{22}^s$ | $-g_{12}$ | $g$ | $c_{12}^0$ |
| 0.0 | 0.25 | 0.25 | 0.0 | 0.50 | 1.0 |
| 0.4 | 0.221 | 0.224 | 0.050 | 0.547 | 1.304 |
| 0.8 | 0.201 | 0.208 | 0.080 | 0.570 | 2.216 |
| 1.2 | 0.191 | 0.201 | 0.098 | 0.589 | 4.040 |
| 1.4 | 0.189 | 0.201 | 0.103 | 0.597 | 5.180 |
| 1.6 | 0.190 | 0.203 | 0.105 | 0.605 | 6.320 |
| 1.8 | 0.193 | 0.208 | 0.105 | 0.612 | 7.460 |
| 2.0 | 0.198 | 0.215 | 0.103 | 0.619 | 8.600 |

$$\chi_{0i}(q,i\omega,n_i)=N_i(0)\left[\frac{\mathrm{Re}\bar{\chi}\left[\frac{i\omega/2E_{Fi}}{q/q_{Fi}}-\frac{q/q_{Fi}}{2}\right]}{q/q_{Fi}}\right], \quad (30)$$

where

$$\bar{\chi}(z)=-2z-(1-z^2)\mathrm{Ln}\left[\frac{z+1}{z-1}\right], \quad (31)$$

$\mathrm{Ln}z=\ln|z|+i\arg(z)$ is the complex logarithm,

$$N_i(0)=\frac{mq_{Fi}}{2\pi^2\hbar^3} \quad (32)$$

is the density of states of the $i$th component per spin at the Fermi surface, and $q_{Fi}$ and $E_{Fi}$ are the Fermi momentum and Fermi energy of the $i$th component with density $n_i$. Next, we use the fluctuation-dissipation theorem to calculate the static correlation functions

$$\langle n_i(\mathbf{q})n_j(-\mathbf{q})\rangle\equiv\Omega n_i\left[\delta_{ij}+\frac{n_j}{n}\gamma_{ij}(r_s,x;q)\right]$$

$$=\frac{\Omega\hbar}{\pi}\int_0^\infty d\omega\,\chi_{ij}^s(q,i\omega), \quad (33)$$

where $\Omega$ is the volume of the EHL and the $\gamma_{ij}(r_s,x;q)$ are the partial static structure factors. The exchange-correlation energy per particle is

$$\epsilon_{\mathrm{xc}}(r_s,x)=\frac{2}{\pi\alpha r_s}\int_0^{r_s}dr_s'\int_0^\infty dq\,\gamma(r_s',x;q), \quad (34)$$

where

$$\gamma(r_s,x;q)=\sum_{i,j=1}^{2}\xi_i\xi_j\frac{n_in_j}{n^2}\gamma_{ij}(r_s,x;q), \quad (35)$$

where $\xi_i=-1$ for electrons and $+1$ for holes. We differentiate this exchange-correlation energy according to Eqs. (24) and (25) and obtain the new values of the $g_{ij}$'s to be used as an input for the next iteration. The whole procedure usually converges within three or four iterations.

We have calculated the $g_{ij}$'s as functions of $r_s$ for several values of mass ratio and degeneracy. Some typical results are shown in Table I. The values of the $g_{ij}$'s are slowly varying functions of $\rho$, which follows from the exchange-correlation energy being almost independent of $\rho$ in the range of interest. Thus, the single case $\rho=6$ is representative of the situation for $1\le\rho\le10$. At small $r_s$, the exchange-correlation energy is dominated by exchange. In this limit, the $g_{ij}$'s can be evaluated exactly from Eqs. (24) and (26) and the result is

$$\lim_{r_s\to0}g_{ii}^s=\frac{1}{4\nu_i^{1/3}},\quad\lim_{r_s\to0}g_{12}=0. \quad (36)$$

From Table I we see that the $r_s$ dependence of the $g_{ij}$'s is also very slight. $g_{11}^s$ and $g_{22}^s$ initially decrease with increasing $r_s$, but $g_{12}$ increases more rapidly so that the important combination

$$g=g_{11}^s+g_{22}^s-2g_{12}^s, \quad (37)$$

which gives the compressibility correction, keeps increasing.

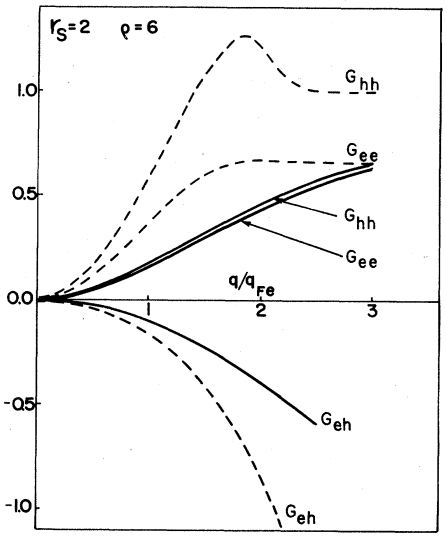


FIG. 1. Spin-symmetric local-field corrections in an EHL: our model (solid line) vs STLS (Ref. 7) (dashed line).

In Fig. 1 we plot our phenomenological $G$'s for typical values of $r_s$ and $\rho$ and compare them with the results of STLS theory. Although the large-$q$ limits of the two sets of curves are practically the same, large differences arise in the small-$q$ region where our local fields are considerably weaker. We recall that STLS theory does not satisfy the compressibility sum rules, whereas our model does: this is a main source of difference between the two results. There are, however, some features of the STLS result, such as the peak in $G_{hh}^s$ or the marked difference between $G_{ee}^s$ and $G_{hh}^s$, which might persist after the small-$q$ behavior has been corrected. Our parametrization is clearly incapable of giving such features. The STLS $G$'s are presumably good for large and intermediate wave vectors since they give accurate values for the correlation energy and the electron-hole enhancement factor. It is very likely, therefore, that our parametrization underestimates the local-field corrections. We shall see in the following that larger local fields give a higher transition temperature. Consequently, our estimate for $T_c$ will be probably smaller than the actual value.

With the self-consistent parameters given in Table I, we have calculated the ground-state energy per $e$-$h$ pair as a function of $r_s$ for various values of $\rho$. The resulting curves are plotted in Fig. 2. The agreement with the STLS result is not perfect but quite satisfactory for mass ratio $\rho$ up to 10. There is a shallow minimum around $r_s=1.9$ which becomes shallower at large values of the mass ratio. The equilibrium $r_s$ is almost independent of $\rho$ when $\nu_1=\nu_2$; it decreases with increasing $\rho$ when $\nu_1>\nu_2$ and increases with $\rho$ when $\nu_1<\nu_2$. The equilibrium values of $r_s$ and of the compressibility enhancement are tabulated in the first two columns of Table IV. For $\rho>10$ the STLS theory does not converge, whereas our model predicts a binding energy that is too large compared to the predictions of more accurate calculations. This bad behavior arises because the hole-hole correlation energy is overestimated. It is therefore not justified to use the

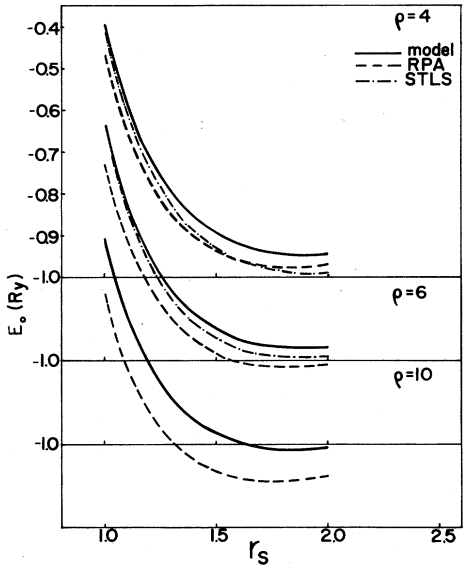


FIG. 2. Ground-state energy of an EHL within our model, in the RPA, and in STLS theory (Ref. 7).

present model for large values of $\rho$.

Consider now the spin-antisymmetric local-field factors $G^a_{ii}(q)$. Since we are neglecting magnetic interactions between electrons and holes, the spin responses of the two components are decoupled from each other. As a first approximation we can treat each component as an independent Coulomb liquid with an effective coupling constant $r_{si}=r_s m_i/\mu$ ($r_{si}$ is the average distance between two particles of the $i$th component measured in units of the Bohr radius of that component). We can therefore use the local-field correction of the electron liquid calculated at the appropriate value of the coupling constant. A simple parametrization of this spin-antisymmetric local-field correction which satisfies the susceptibility sum rule for the electron liquid has been recently proposed by Pines. Its form is

$$G^a(q)=\frac{1}{2}\left[\frac{q^2}{q^2+q^2_{\uparrow\uparrow}}-\frac{q^2}{q^2+q^2_{\uparrow\downarrow}}\right], \tag{38}$$

where $q_{\uparrow\uparrow}$ and $q_{\uparrow\downarrow}$ are $r_s$-dependent parameters which are given in Ref. 17 and Table II. In our effective interaction we shall use

$$G^a_{ii}(q)=\frac{1}{\nu_i}G^a(q)\Big|_{r_s m_i/\mu}, \tag{39}$$

which is consistent with our definition of $G^a_{ii}$ [Eq. (9)]. We also define

$$g^a_{ii}\equiv\lim_{q\to 0}\left[\frac{G^a_{ii}(q)}{(q/q_F)^2}\right]. \tag{40}$$

Having completed the phenomenological construction of the local-field corrections, we can now calculate the effective interaction and examine its consequences.

TABLE II. Parameters of the spin-antisymmetric local-field corrections [Eqs. (38)–(40)]: $q_{\uparrow\uparrow}$ and $q_{\uparrow\downarrow}$ are taken from Ref. 17, and $g^a=[(q_F/q_{\uparrow\uparrow})^2-(q_F/q_{\uparrow\downarrow})^2]/2$.

| $r_s$ | $q_{\uparrow\uparrow}/q_F$ | $q_{\uparrow\downarrow}/q_F$ | $g^a$ |
|---|---|---|---|
| 1 | 1.47 | 4.12 | 0.202 |
| 2 | 1.50 | 3.30 | 0.176 |
| 3 | 1.52 | 2.93 | 0.158 |
| 4 | 1.53 | 2.71 | 0.146 |
| 5 | 1.54 | 2.56 | 0.135 |
| 10 | 1.57 | 2.19 | 0.099 |
| 15 | 1.60 | 2.02 | 0.073 |
| 20 | 1.60 | 1.91 | 0.058 |

## IV. PROPERTIES OF THE EFFECTIVE INTERACTION

Consider the small-$q$ limit of the static effective interaction in the singlet state of two electrons:

$$\lim_{q\to 0}\lim_{\omega\to 0}[V_{\rm eff}(q,\omega)]=\frac{4\pi e^2}{q_F^2}\left[\frac{1}{2\gamma_1}+g^s_{11}+(2\nu_1+1)\frac{2\gamma_1(g^a_{11})^2}{1-2\gamma_1 g^a_{11}}-\left[\frac{1}{2\gamma_1}\right]^2\frac{2\gamma}{1-2\gamma g}\right], \tag{41}$$

with $g$ defined in Eq. (37). The first two terms within the large square brackets correspond to the spin-independent part of the purely electronic interaction, the third term corresponds to the spin-fluctuation part of the interaction, and the last term—which is attractive—corresponds to the hole-mediated interaction. The multiplying factor $(1/2\gamma_1)^2$ of the latter corresponds to the small-$q$ limit of $v^2_{eh}(q,0)$. We have seen that the denominator $1-2\gamma g$ of the last term is equal to the compressibility ratio $\kappa_f/\kappa$ and tends to zero as $r_s\to r_{sc}\cong 2.5$ ($\nu_1=\nu_2=1$). Since in the same density range the other denominator, $1-2\gamma_1 g^a_{11}$, is always close to unity, we conclude that the hole-mediated attraction must become the dominant term as $r_s$ approaches $r_{sc}$. The question is whether the equilibrium $r_s$ is large enough for this to happen. The answer to this question is given in Figs. 3 and 4. We have chosen typical values of the parameters, $\rho=6$ and $r_s=1.9$, and the local-field factors calculated in the preceding section. Not only is the effective interaction attractive in the limit of Eq. (41), it is also attractive at finite wave vectors up to $q\sim 2q_F$ and frequencies up to $\omega\sim E_{Fh}$.

It is interesting to compare this result with that of the RPA and with the dielectric interaction $v/\epsilon$ given in Eq. (11). The small-$q$ limit of the RPA is obtained by setting all the $g$'s equal to zero in Eq. (41). What one obtains in this way is the Thomas-Fermi limit, which is always

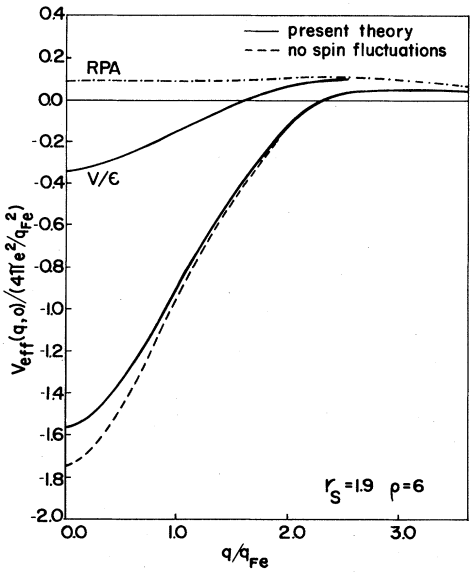


FIG. 3. Static effective interaction between two electrons in an EHL in our theory (with and without spin fluctuations), in the RPA, and in the dielectric approximation. The electrons are assumed to be in a singlet state.

repulsive (this is also, incidentally, the small-$r_s$ limit of our interaction). The RPA interaction at finite $q$ is shown as a dashed-dotted line in Fig. 3. The dielectric interaction $v/\epsilon$ can be written, in the small-$q$ limit, as

$$\lim_{q\to 0}\lim_{\omega\to 0}\frac{v}{\epsilon(q,\omega)}=\frac{4\pi e^2}{q_F^2}\left[\frac{1}{2\gamma_1}-g_{11}^s-\left[\frac{1}{2\gamma_1}-g_{11}^s+g_{12}\right]^2\frac{2\gamma}{1-2\gamma g}\right]. \tag{42}$$

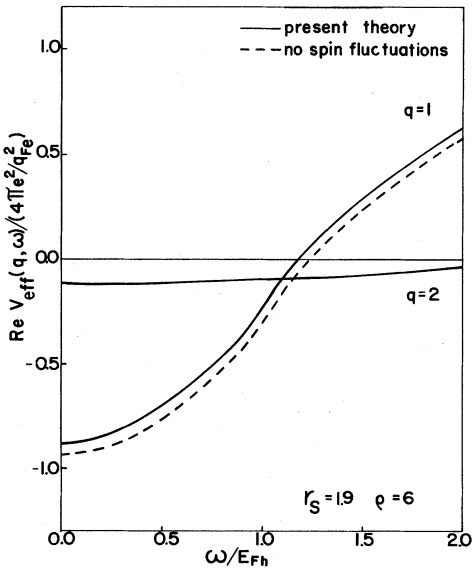


FIG. 4. Frequency dependence of the single-state effective interaction between two electrons in an EHL in our theory (with and without spin fluctuations) for $q=q_{F1}$ and $q=2q_{F1}$.

Both the repulsive and attractive terms are reduced relative to Eq. (41), but the second effect dominates and the net attraction is weakened (see Fig. 3).

A very interesting difference between our interaction and the dielectric one is that the latter is the same between two electrons as it is between two holes, whereas ours is not. The limiting forms of the effective interactions between two holes can be simply obtained by interchanging the subscripts 1 and 2 in Eqs. (41) and (42). Equation (42) can be easily proved to be invariant under such a transformation. This would lead one to the erroneous conclusion that superconductivity is more likely to occur within the hole subsystem because of its larger density of states at the Fermi surface. In our case, instead, the effective interaction between two holes is always more repulsive than the effective interaction between two electrons: it is, in fact, repulsive for all $q$'s for the values of the parameters $r_s=1.9$ and $\rho=6$. In Fig. 5 we have plotted the static effective interaction between two holes in the singlet state [i.e., from Eq. (12a) with $1\leftrightarrow 2$], in the triplet state (where the prefactor 3 of the spin-fluctuation term is replaced by $-1$ as detailed in Appendix A), and without spin fluctuations. These three results are widely different and show that spin fluctuations play an extremely important role in the hole-hole interaction. In contrast to this, the electron-electron interaction in an EHL is almost unaffected by spin fluctuations, as shown in Fig. 3. This is easy to understand because the holes, with their large effective coupling constant ($r_{sh}\sim 15$ when $r_s\sim 2$), are nearer than the electrons to a ferromagnetic instability. Mathematically, this fact is expressed by the smallness of the denominator $1-2\gamma_2 g_{22}^a$ in Eq. (41) for the holes. The enhanced spin fluctuations due to the proximity of such an instability determine a repulsive interaction in the singlet state or an attractive one in the triplet state. In the latter case the total interaction can even become attractive if the ferromagnetic instability is sufficiently near: one can have, in principle, triplet superconductivity. In an EHL with $\rho\sim 10$ the attractive interaction between two

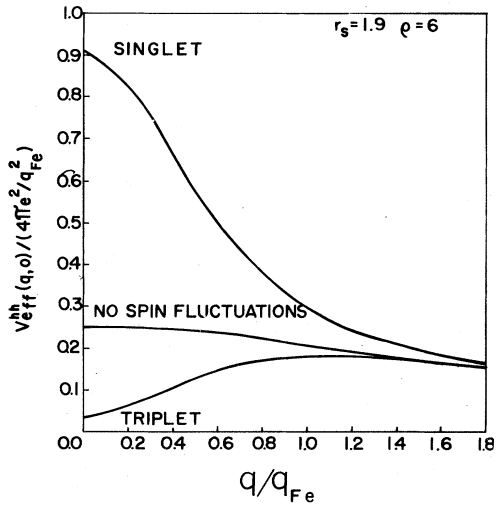


FIG. 5. Static effective interaction between two holes in an EHL, with spin fluctuations in the singlet or in the triplet state and without spin fluctuations.

holes in the triplet state, even if present, remains much smaller than the attractive interaction between two electrons in the singlet state. The reason is that the Fermi liquid of heavy holes, due to its large density of low-lying excitations, screens itself very effectively from the electrons which could mediate an attractive interaction [the last term of Eq. (41) tends to zero for increasing mass ratio]. At the same time, the spin-fluctuation effect is not strong enough at this mass ratio. We conclude that only electrons can form Cooper pairs in the singlet state, while the hole subsystem remains normal.

Having thus clarified the general features of the interaction, we examine more closely the various parameters that determine the value of the critical temperature.

### A. Attraction parameter λ

The attraction parameter λ is defined as the $s$-wave average over the Fermi surface of electrons of the static interaction $U_h(q,0)$ [Eq. (12c)] times the density of states $N_1(0)$:

$$\lambda = N_1(0) \int_0^{2q_{F1}} dq \frac{q}{2q_{F1}^2} v_{eh}^2(q,0) \, | \chi_{22}^s(q,0) | \ , \tag{43}$$

where $v_{eh}$ and $\chi_{22}^s$ are defined in Eqs. (13c) and (13d), respectively. The intimate connection between λ and the spectral distribution of density-fluctuation excitations is due to the dispersion relation

$$| \chi_{22}^s(q,0) | = \frac{2}{\pi} \int_0^\infty \frac{| \mathrm{Im}\chi_{22}^s(q, \omega + i\delta) |}{\omega} d\omega \ . \tag{44}$$

Clearly, it is the low-frequency part of the spectrum $\mathrm{Im}\chi^s(q,\omega)$ that gives the dominant contribution to the static polarizability and to λ. This part of the spectrum can, in turn, be separated, more or less distinctly, into two parts, the lower-frequency one corresponding to pair excitations from the hole Fermi sea and the higher-frequency one corresponding to the acoustic plasmon. Again, we can say that the former contribution will be decisive in determining the value of λ. In Figs. 6(a)–6(c) we plot the density-fluctuation spectrum $\mathrm{Im}\chi_{22}^s(q,\omega)$ with and without local-field corrections, the latter being, by definition, the RPA. The differences between these two sets of curves are striking. In the RPA most of the spectral weight is in the collective mode, just above the upper limit of the pair continuum (indicated by arrows in Fig. 6); even at $q = 2q_F$, where the acoustic plasmon has disappeared, the spectral weight tends to concentrate near the upper cutoff. On the other hand, when local-field corrections are included, the collective mode is practically suppressed and the spectral weight shifts to the pair-excitation region. Physically, this rather drastic change reflects the softness of the liquid due to the exchange and correlation effects. At the equilibrium $r_s$ considered in the figures, the pair-excitation spectrum, although enhanced, is still rather broad. At larger $r_s$—as the compressional instability is approached—the spectrum becomes more and more peaked on the low-energy side. At the same time, λ grows larger and larger, tending logarithmically to infinity at the critical $r_s$. Thus, proper inclusion of the local-field corrections has revealed the existence of a low-frequency

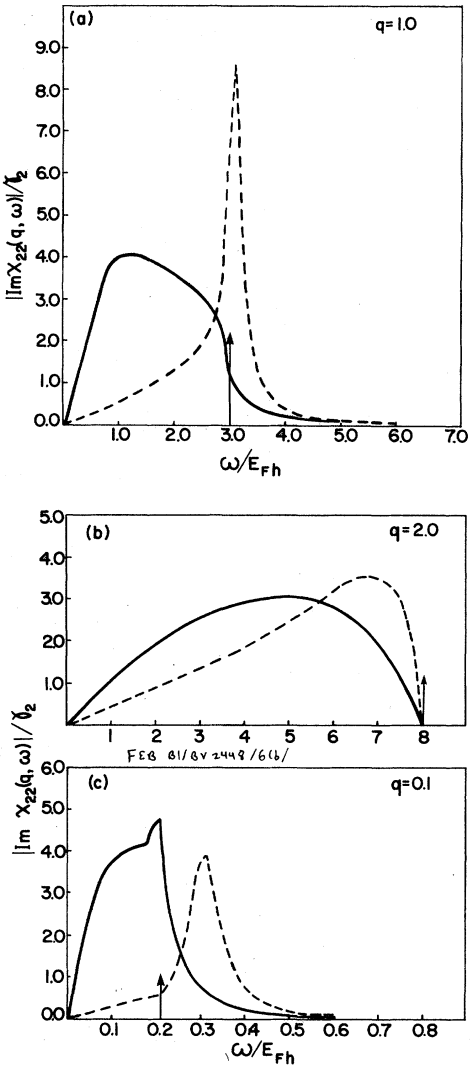


FIG. 6. Density-fluctuation spectrum of the holes in the RPA (dashed line) and GRPA (solid line) for (a) $q = q_F$, (b) $q = 2q_F$, and (c) $q = 0.1q_F$. Parameters are $r_s = 1.9$, $\rho = 6$, and $\nu_1 = \nu_2 = 1$. Arrows indicate the upper limit of the pair continuum.

attractive mechanism mediated by correlated pair excitations and much more effective than the usually proposed collective mechanism.

The spectra shown in Fig. 6 explain why our theory predicts superconductivity in the EHL, whereas the RPA does not, but they still do not explain why the dielectric interaction $v/\epsilon$ should not work equally well. The spectral functions are the same in the two cases, and any difference can only arise due to the effective potential coupling electrons to holes. In the case of the dielectric interaction this potential is

$$v_{eh}^D(q) = v_q \frac{1 - (\psi_{11}^s - \psi_{12})\chi_{01}}{1 - \psi_{11}^s \chi_{01}} \ , \tag{45}$$

and it is much weaker than our $v_{eh}(q)$ or, for that matter, the RPA $v_{eh}(q)$. The situation is summarized in Fig. 7.

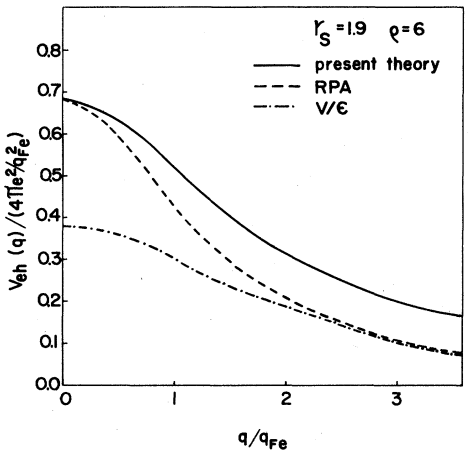


FIG. 7. Static electron-hole effective potential in our theory, in the RPA, and in the dielectric approximation.

Notice that the small-$q$ and -$\omega$ limit of Eq. (45), which is the term in large round parentheses in Eq. (42) is much smaller than the correct Heine-Nozières-Wilkins limit which both our theory and the RPA satisfy. The difficulty with the dielectric interaction originates from including exchange-correlation effects within the medium (the local-field factors in the polarizabilities), but not between the particles and the medium (vertex corrections). Note, also, that our curve for $v_{eh}(q)$ still lies slightly higher than that of the RPA because of the combined effect of vertex corrections and the electron-hole enhancement factor.

In Fig. 8 we plot our calculated values of $\lambda$ versus $r_s$ for $\nu_1=\nu_2=1$ and $\rho=3$ and 10. The behavior of these curves versus $r_s$ has already been discussed; their dependence on mass ratio and degeneracy remains to be explained. The fact that $\lambda$ increases with $\rho$ is mostly due to the increase in equilibrium compressibility. We have found that the compressibility ratio $\kappa_f/\kappa$ at equilibrium density varies from $\sim 0.25$ at $\rho=1$ to $\sim 0.20$ at $\rho=10$. This accounts for most of the increase of $\lambda$ with $\rho$. There is also another effect contributing to this increase: changing $\rho$ at constant $r_s$ means that the masses of electrons and holes are changed according to the law $m_1=\mu(1+1/\rho)$ and $m_2=\mu(1+\rho)$, where the reduced mass $\mu$ is kept constant so that the density, the effective Bohr radius, and the effective rydberg do not change. When $\rho$ is increased, the electron mass $m_1$ decreases and so does the electronic density of states at the Fermi surface. Consequently, there is less electronic screening between electrons and holes, and the electron-hole potential is strengthened.

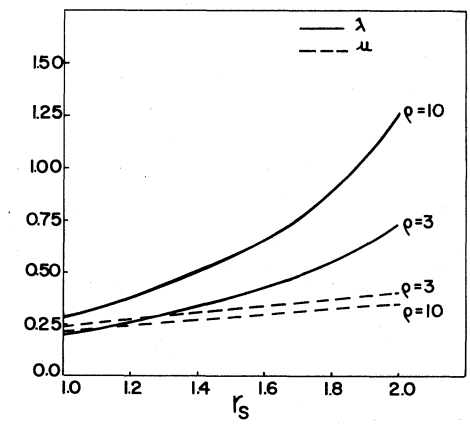


FIG. 8. Interaction parameters $\lambda$ and $\mu$ vs $r_s$ for $\rho=3$ and 10, and $\nu_1=\nu_2=1$ (also see Table III).

The dependence of $\lambda$ on valley degeneracy can also be understood after similar considerations. We first consider the effect of increasing the number of hole valleys. The total density of states of the holes at the Fermi surface is proportional to $\nu_2^{2/3}$. This gives an extra factor $\nu_2^{2/3}$ in the Lindhard function $\chi_{02}(q,0)$ appearing in both the numerator and the denominator of the expression for the polarizability of the holes, $\chi^s_{22}(q,0)$. As a consequence, the polarizability of the holes increases, although slightly, and this gives a larger $\lambda$. We now consider the effect of increasing the number of electron valleys. Since intervalley scattering due to Coulomb interactions is negligible, as already remarked in Sec. II, it is clear that the density of states in Eq. (43) is the density of states of electrons in *one* band. At the same time, however, *all* electrons contribute to the screening of the electron-hole interaction, i.e., the Lindhard polarizability $\chi_{01}(q,0)$ has an extra factor $\nu_1^{2/3}$ coming from the total density of states of the electrons. This results in a drastic reduction of $\lambda$. In Table III we give the values of $\lambda$ for $\rho=10$, $\nu_1=4$, and $\nu_2=1$. In this case, both the equilibrium $r_s$ and critical $r_s$ are much smaller than in the nondegenerate case: we find $r_{s0}\cong 1.0$ and $r_{sc}\cong 1.25$. One should not therefore be deceived by the fact that the values of $\lambda$ are larger than in the nondegenerate case for the same value of $r_s$. This is simply due to the fact that the system is nearer to the compressional instability than in the nondegenerate case at the same $r_s$. Comparing the equilibrium values of $\lambda$ (Table IV), we find $\lambda=0.27$ at $\rho=10$, much less than the value, $\lambda=1.05$, in the nondegenerate case. This is what one should expect from the argument given above.

In the theory of the electron-phonon interaction, the pa-

TABLE III. Interaction parameters $\lambda$, $\mu$, and $\omega_0/E_{Fh}$ vs $r_s$ at $\rho=10$.

| $r_s$ | $\lambda$ | $\mu$ | $\omega_0/E_{Fh}$ |
|---|---|---|---|
| | $\nu_1=1$, $\nu_2=1$, $\rho=10$ | | |
| 1.0 | 0.286 | 0.212 | 1.301 |
| 1.5 | 0.575 | 0.285 | 1.166 |
| 2.0 | 1.267 | 0.353 | 0.772 |
| | $\nu_1=1$, $\nu_2=4$, $\rho=10$ | | |
| 1.0 | 0.293 | 0.212 | 3.603 |
| 1.5 | 0.591 | 0.285 | 3.225 |
| 2.0 | 1.418 | 0.353 | 1.909 |
| | $\nu_1=4$, $\nu_2=1$, $\rho=10$ | | |
| 1.0 | 0.269 | 0.148 | 0.512 |
| 1.1 | 0.359 | 0.159 | 0.392 |
| 1.2 | 0.564 | 0.171 | 0.216 |

TABLE IV. Equilibrium values of $r_s$, inverse compressibility enhancement, interaction parameters, and superconducting $T_c$ vs $\rho$.

| $\rho$ | $r_{s0}$ | $\kappa_f/\kappa$ | $\lambda_0$ | $\mu_0$ | $\omega_0/E_{Fh}$ | $T_c(\epsilon_\infty^2/\mu)$ (K) |
|---|---|---|---|---|---|---|
| | | | $\nu_1=1,\ \nu_2=1$ | | | |
| 3 | 1.9 | 0.244 | 0.634 | 0.385 | 0.550 | 4.38 |
| 6 | 1.9 | 0.222 | 0.811 | 0.355 | 0.711 | 215.34 |
| 10 | 1.9 | 0.201 | 1.052 | 0.339 | 0.879 | 577.64 |
| | | | $\nu_1=1,\ \nu_2=4$ | | | |
| 3 | 1.72 | 0.248 | 0.636 | 0.358 | 1.305 | 13.06 |
| 6 | 1.77 | 0.247 | 0.767 | 0.335 | 1.955 | 239.83 |
| 10 | 1.80 | 0.229 | 0.944 | 0.326 | 2.577 | 590.82 |
| | | | $\nu_1=4,\ \nu_2=1$ | | | |
| 8 | 1.03 | 0.226 | 0.257 | 0.151 | 0.462 | 0.409 |
| 10 | 0.98 | 0.24 | 0.256 | 0.145 | 0.533 | 0.796 |

rameter $\lambda$ is usually related to the mass enhancement of electrons at the Fermi surface: $m^*/m \cong 1+\lambda$. This formula is derived under the hypothesis of Migdal's theorem and therefore has only approximate validity here. Preliminary calculations show that the mass enhancement for electrons in an EHL is better represented by the formula $m^*/m \cong 1+\lambda/(1+\mu)$, where $\mu$ is the Coulomb repulsion parameter to be discussed in the next section. The mass renormalization of the holes is, instead, very small. We have used, in our calculations, effective masses determined by band structure only. This is a reasonable approximation, at least for the calculation of the polarizability, since, as discussed, for example, by Schrieffer *et al.*,[21] the low-frequency polarizability of a Fermi liquid is essentially unaffected by a self-energy correction which varies on a scale much smaller than the Fermi energy (although mass renormalization may be large). In our case, the relevant self-energy varies on the scale of the Fermi energy of the holes and thus should not affect the polarizability of the electrons too much. While this takes care of the renormalization of the "internal" electrons, there is still an important effect of renormalization of the "external" electrons which has not been taken into account so far. We shall worry about this effect when we come to the calculation of the critical temperature.

### B. Repulsion parameter $\mu$

The repulsion parameter $\mu$ is defined as the $s$-wave average over the Fermi surface of the electrons of the static interaction $U_c(q,0)$ [Eq. (12b)] times the density of states $N_1(0)$. In dimensionless units,

$$\mu = N_1(0) \int_0^{2q_{F1}} dq\,(q/2q_{F1}^2)\,U_c(q,0)\ . \tag{46}$$

The static interaction $U_c(q,0)$ is plotted in Fig. 9 for various approximations. Our result (solid curve) lies considerably above the RPA curve (dashed-double-dotted line). Using the dielectric interaction of Eq. (11), the curve for $U_c(q,0)$ (dashed-dotted line) would, instead, lie well below the RPA curve.

The effective interaction $U_c(q,0)$, with the local-field correction $G_{11}^s(q)$ replaced by the one appropriate for the electron liquid, can be used to calculate the electron-electron contribution to the thermal resistivity of a simple metal. Kukkonen and Smith[22] calculated this quantity using the Thomas-Fermi screened Coulomb interaction (which is not very different from the RPA) and obtained a result that was smaller than that of experiment by a factor of 7. This is a clear indication of the fact that the RPA underestimates the effective electron-electron interaction. Our effective interaction, being stronger than that in the RPA, would improve the agreement with experimental values, whereas the dielectric interaction would make it worse. Here, again, as in the case of the effective electron-hole potential, we find that using a better dielectric function without accounting for vertex corrections and ladder diagrams makes a poorer approximation than the RPA.

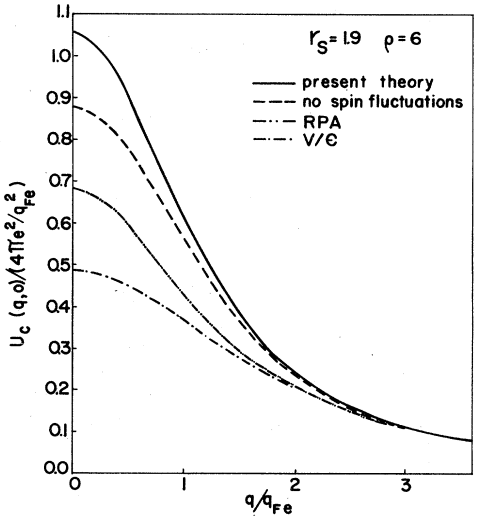


FIG. 9. Purely electronic part of the interaction between two electrons in a singlet in our theory (with and without spin fluctuations), in the RPA, and in the dielectric approximation.

In Fig. 9 we have also plotted $U_c(q,0)$ without the spin-fluctuation term (dashed line). This term, which is repulsive, is not very large at EHL densities and accounts for less than 20% of the interaction at very small $q$.

The values of $\mu$ calculated from Eq. (46) are plotted in Fig. 8 for $\nu_1=\nu_2=1$ and $\rho=3$ and 10. This parameter depends very slightly on $r_s$, $\rho$, and valley degeneracy (see Table III). It increases with increasing $r_s$ and decreases with increasing $\rho$. Its value at equilibrium density varies from $\mu_0=0.42$ at $\rho=2$ to $\mu_0=0.34$ at $\rho=10$ in the nondegenerate case. These values are substantially larger than the Thomas-Fermi values ($\mu_0<0.25$) and arise from the combined effect of vertex corrections and spin fluctuations.

### C. Characteristic frequency $\omega_0$

The characteristic frequency $\omega_0$ is defined[23] as the logarithmic average over the effective electron-hole coupling function $\alpha^2F(\omega)/\omega$:

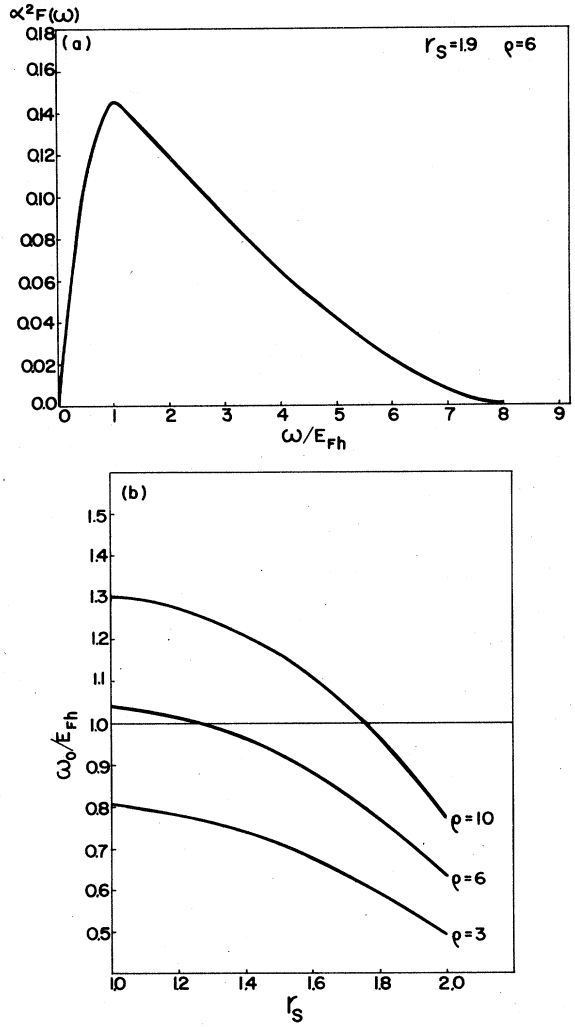


FIG. 10. (a) Typical shape of the electron-hole coupling function $\alpha^2F(\omega)$ in an EHL; (b) characteristic frequency $\omega_0$ from Eq. (47) vs $r_s$ for various values of $\rho$ (also see Table III).

$$\omega_0=\exp\left[\frac{2}{\lambda}\int_0^\infty d\omega\left[\frac{\ln\omega}{\omega}\alpha^2F(\omega)\right]\right], \tag{47}$$

where

$$\alpha^2F(\omega)=N_1(0)\int_0^{2q_{F1}}dq\frac{q}{2q_{F1}^2}\frac{v_{eh}^2(q,\omega)}{\pi}\,|\,\mathrm{Im}\chi_{22}^s(q,\omega+i\delta)\,| \tag{48}$$

is the analog of the electron-phonon coupling function, i.e., a weighted average of the density-fluctuation spectrum of the holes, with wave vectors $q$ spanning the Fermi surface of the electrons, and the square of the electron-hole potential as a weighting function. A typical plot of $\alpha^2F(\omega)$ is shown in Fig. 10(a). The function has a peak around the Fermi energy of the holes and then decreases slowly, up to the maximum energy of a pair excitation with wave vector $2q_F$, which is $\omega_m=8E_{Fh}$. This value of the energy is the natural cutoff to be used as an upper limit in the integral of Eq. (47). With this cutoff, the sum rule

$$\lambda=2\int_0^\infty d\omega\,\omega^{-1}\alpha^2F(\omega) \tag{49}$$

is satisfied with an accuracy of a fraction of percent.

The electron-hole coupling function of Eq. (48) is formally identical to the "Eliashberg function" used by Jaffe and Ashcroft[12] in their calculation of superconducting $T_c$ in liquid metallic hydrogen. The actual shape of our curve is, however, very different from that for liquid metallic hydrogen. In the latter case, $\alpha^2F(\omega)$ has a strong acoustic-plasmon peak just below the upper cutoff (height of the peak $>2.5$ according to JA). The pair continuum from the Fermi sea of the protons appears as a low-frequency plateau with average height $<0.3$. In our case there is no contribution from the acoustic plasmon and the peak around $E_{Fh}$ has strength $<0.2$.

In Fig. 10(b) we plot the value of $\omega_0$ as a function of $r_s$ for various values of $\rho$. As $r_s$ is increased from 1 to 2, $\omega_0$ decreases from a value greater than $E_{Fh}$ to a fraction of $E_{Fh}$. This is not surprising because, as the system becomes more compressible, its characteristic frequency is expected to decrease. As $\rho$ increases, the main change in the density-fluctuation spectrum is the growth of the acoustic-plasmon peak on the high-energy side: as a consequence, $\omega_0$ increases. It is worth noting that the dependence of $\omega_0$ on $\rho$ is much stronger at small $r_s$ than at large $r_s$. This observation confirms our interpretation of the effect, since the acoustic plasmon has a larger frequency at smaller $r_s$ and is also better defined.

The general features discussed above remain valid in the case of a multivalley system. The only difference concerns the value of the ratio $\omega_0/E_{Fh}$. If $\nu_1=1$ but $\nu_2>1$, then $E_{Fh}=\hbar^2q_F^2/2m_h\nu_2^{2/3}$ decreases, but $\omega_0$ is still fixed by the Fermi momentum of the electrons $q_{Fe}=q_F$. Thus the ratio $\omega_0/E_{Fh}$ increases. On the other hand, if $\nu_2=1$ but $\nu_1>1$, then $E_{Fh}$ does not change, but $\omega_0$ decreases because $q_{Fe}=q_F/\nu_1^{1/3}$. Thus the ratio $\omega_0/E_{Fh}$ decreases.

## V. CRITICAL TEMPERATURE

The superconducting transition temperature $T_c$ is determined by the equation

$$F(p,i\omega_n)=-B(p,i\omega_n)T_c\sum_{m,\mathbf{k}}V_{\rm eff}(\mathbf{p}-\mathbf{k};i\omega_n-i\omega_m)\times F(\mathbf{k},i\omega_m)\ , \tag{50}$$

where $F(p,i\omega_n)$ is the anomalous Green's function for electrons in the superconducting state, $V_{\rm eff}(q,i\omega_n)$ is the normal-state effective interaction, irreducible in the particle-particle channel, and

$$B(\mathbf{p},i\omega_n)=G(\mathbf{p},i\omega_n)G(-\mathbf{p},-i\omega_n)\ , \tag{51}$$

where $G(\mathbf{p},i\omega_n)$ is the normal electron Green's function and the $\omega_n=(2n+1)\pi T_c$ are Matsubara frequencies. A complete solution of Eq. (50) is a difficult numerical task that we do not attempt in this paper. However, in view of the fact that the net interaction is strongly attractive over a comparatively large range of wave vectors and frequencies, a reasonable estimate of $T_c$ can be obtained from a McMillan[24] type of formula:

$$T_c\cong\omega_0\exp\left[-\frac{1}{\lambda^*-\mu^*}\right]\ , \tag{52a}$$

where the renormalized parameters $\lambda^*$ and $\mu^*$ are defined as

$$\lambda^*=\lambda/(\lambda+1) \tag{52b}$$

and

$$\mu^*=\frac{\mu}{1+\mu\ln\rho}\ . \tag{52c}$$

This approximate formula, which clearly can only be used if $\lambda^*>\mu^*$, can be obtained from a two—square-well solution of the renormalized version of the equation proposed by Kirzhnits, Maksimov, and Khomskii (KMK).[25] These authors use a particularly simple ansatz for the spectral function associated with the anomalous Green's function, namely

$$f(\mathbf{p},\omega)\equiv-\frac{1}{\pi}\mathrm{Im}F(p,\omega+i\delta)\cong\frac{1}{2|\epsilon_p|}[\delta(\omega-\epsilon_p)-\delta(\omega+\epsilon_p)]\phi(p)\ , \tag{53}$$

where the $\epsilon_p$ are free-electron energies relative to the chemical potential. In this way they are able to transform Eq. (50) into a manageable one-dimensional equation for the auxiliary function $\phi(p)$. The KMK equation, however, neglects strong-coupling corrections. In particular, the external Green's functions of Eq. (51) are replaced, in their derivation, by noninteracting Green's functions. We have seen in Sec. IV that mass renormalization can be quite large for electrons in an EHL ($>50\%$) and we know that the critical temperature is very sensitive to this effect. We remedy the situation by using a modified KMK equation which is derived in the manner of the original one, but with a Green's function of the form

$$G(\mathbf{p},i\omega_n)=\frac{Z^{-1}}{i\omega_n-\epsilon_p^*}\ , \tag{54}$$

where $Z=m^*/m\cong1+\lambda$ and $\epsilon_p^*$ is the free-particle energy corresponding to the mass $m^*$ which must also enter the KMK ansatz, Eq. (53). In this way we hope to have retained at least the most important renormalization effects. Some details on the derivation of Eq. (52a) are given in Appendix C.

In Fig. 11(a) we have plotted the transition temperature at equilibrium density as a function of the mass ratio. Using the relation

$$1\ \mathrm{Ry}^*=(\mu/\epsilon_\infty^2)\ \mathrm{Ry}\cong(\mu/\epsilon_\infty^2)(1.57\times10^5\ \mathrm{K})\ ,$$

we give $T_c$ in units of $(\mu/\epsilon_\infty^2)$ K. The solid line corresponds to the complete result for $\nu_1=\nu_2=1$ and $r_{s0}=1.9$. The dashed line denotes the result obtained without including spin fluctuations. Results for different degeneracies are also presented in Table IV. The most important

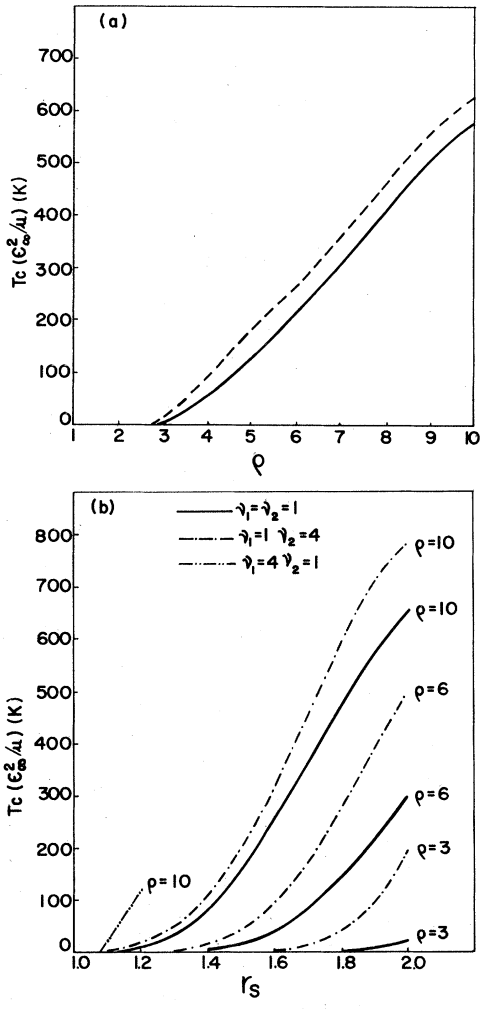


FIG. 11. (a) Superconducting transition temperature of an EHL at equilibrium density vs $\rho$ for $\nu_1=\nu_2=1$ (solid line). The dashed line is the result of our theory when spin fluctuations are *not* included. (b) Superconducting transition temperature of an EHL vs $r_s$ for various values of $\rho$ and valley degeneracy.

feature of these results is what we might call the "inverse isotope effect," or the fact that $T_c$ increases with increasing mass of the holes. This effect follows from the behavior of the interaction parameters $\lambda$ and $\mu$ versus $\rho$, as discussed in Sec. IV. There we saw that $\lambda$ increases and $\mu$ decreases with increasing $\rho$ at fixed $r_s$. The decrease of $\mu^*$ is even faster than that of $\mu$, due to the $\ln\rho$ term in the denominator of Eq. (52c). At the same time, $\omega_0$ decreases because $E_{Fh}\sim 1/\rho$. The behavior of $T_c$ with increasing $\rho$ is, therefore, determined by the competition of two effects: the increase of the difference $\lambda^*-\mu^*$ in the exponential factor and the decrease of the prefactor frequency $\omega_0\sim E_{Fh}\sim 1/\rho$. For the moderate values of $\rho$ that we are considering, the first effect dominates and one finds a 2-order-of-magnitude increase in $T_c$ for $\rho$ varying from 3 to 10. At much larger values of the mass ratio, the parameters $\lambda$ and $\mu$ should essentially saturate and $\omega_0$ should begin to vary as $\rho^{-1/2}$ as the acoustic-plasmon mechanism becomes operative: the usual isotope effect should then be recovered. For $\rho<3$ the transition temperature falls rapidly to zero. Thus a relatively large mass ratio is an important condition in achieving a reasonable value of $T_c$. As an example, we have considered the case of CdS, a direct-band-gap semiconductor with one electron valley and one hole valley, $\rho\cong 6$ and $\mu/\epsilon_\infty^2\cong 0.0046$.[26] We find $T_c\cong 1$ K. In the case of AgBr, an indirect-band-gap semiconductor with one electron valley and four hole valleys, $\rho\cong 3$ and $\mu/\epsilon_\infty^2\cong 0.0077$,[26] we find $T_c\cong 0.1$ K. Note that the valley degeneracy of the holes increases $T_c$ due to the larger polarizability of the holes. Valley degeneracy of the electrons, instead, causes a dramatic drop in $T_c$, since the attraction parameter $\lambda$ is considerably reduced.

In Fig. 11(b) we have plotted $T_c$ as a function of $r_s$ for various values of $\rho$ and valley degeneracy. Here, again, there is competition between the increase of $\lambda^*-\mu^*$ and the decrease of $\omega_0\sim E_{Fh}\sim 1/r_s^2$ Ry$^*$ with increasing $r_s$. Once again, the first effect dominates and one finds the sharply increasing curves of Fig. 11(b). This behavior is the opposite of that predicted by other authors[27,28] working with the "jellium model."

Using the BCS relation $\Delta(0)\cong 1.75 k_B T_c$ for the zero-temperature superconducting gap, we can estimate the order of magnitude of the coherence length:

$$\xi_0=\frac{\hbar V_{F1}}{\Delta(0)}\cong\frac{\mu}{m_1}\frac{1}{\alpha r_s}\frac{1\text{ Ry}^*}{T_c}a_0^*\ , \tag{55}$$

where $V_{F1}$ is the Fermi velocity of the electrons. For $T_c$ of the order of $10^{-3}$ Ry$^*$, we find $\xi_0\sim 10^3 a_0^*$, which is about 10 times larger than the size of an ordinary EHL droplet. The London penetration depth at $T=0$ is

$$\delta_0=\frac{c}{\omega_p}\cong 80\epsilon_\infty r_2^{3/2}a_0^*\ . \tag{56}$$

This is also of the order of $10^3 a_0^*$ for $\epsilon_\infty<10$. Thus, the two length scales are comparable and the possibility arises that EHL is a type-II superconductor. Our calculations are not sufficiently accurate to allow a definite conclusion on this point. Notice, finally, that $T_c\ll\omega_0\sim E_{Fh}$, which justifies our assumption of neglecting the temperature dependence of $\chi_0$'s and $G$'s throughout the paper.

## VI. CRITIQUE AND CONCLUSION

In this paper we have calculated the superconducting transition temperature of an EHL in a model semiconductor and found that, for reasonable values of density and mass ratio, it falls within the observable range ($T_c\sim 1$ K). This conclusion was reached by using an effective interaction which goes beyond the RPA in dealing with exchange and correlation effects. Such effects cannot be simply treated by a screened interaction where the dielectric function includes local-field corrections: it is necessary, instead, to modify the form of the interaction to allow for vertex corrections and particle-hole ladder diagrams. The latter are expressed in our scheme in terms of local-field corrections and play a decisive role in determining the value of $T_c$.

Let us now examine the approximations which have been used in this paper in order to simplify the calculations. There are two main approximations: the first concerns the structure of the local-field corrections and the second, the evaluation of $T_c$ by McMillan's formula. Our approach to the local-field corrections is entirely phenomenological. In essence, we used the fact that in the small-$q$ limit the $G$'s can be calculated from the knowledge of the exchange-correlation energy, while in the large-$q$ limit they can be related, according to previous theories,[6,7] to the pair correlation function at zero separation. We have proposed a simple formula, reminiscent of Hubbard approximation, to interpolate between the two limits. We have compared our $G$'s with those of STLS theory. Although the latter are not reliable at small $q$ (failing to satisfy the compressibility sum rule), they should become more reliable at larger $q$. If this is the case, we can conclude that our model underestimates the local-field corrections at intermediate wave vectors; in particular, it does not give any of the peaks which appear in STLS and other theories. Now we have seen that larger fields will not do any harm to superconductivity, but rather will increase the transition temperature. There is, of course, the possibility that one of the local fields becomes so large as to drive a finite-$q$ instability [charge-density wave (CDW)] in the EHL (See Appendix B). In this case our form of the effective interaction would break down at the transition point and should be replaced by another one with the polarizability appropriate to the CDW state. The breakdown of the computational scheme does not mean that superconductivity is suppressed: on the contrary, $T_c$ should vary continuously through the transition point. We now turn to another aspect of our approximation to the $G$'s, that is, the neglect of their frequency dependence and imaginary parts. Unfortunately, our understanding of the dynamic local-field correction is still at a preliminary stage. Among the few papers which address this difficult problem, we mention those by Holas, Aravind, and Singwi[29] based on kinetic equations and first-order perturbation theory, respectively. These two rather different methods agree in giving a local-field correction which is almost purely real and practically flat as a function of frequency up to the Fermi energy. It is for this reason that we decided to use the static limit of the $G$'s in our calculations.

Our calculation of $T_c$ from Eq. (52) is certainly a very simple one and should be regarded as a semiquantitative estimate. First, we put all the strong-coupling effects in the renormalization factor $Z=1+\lambda$ in the electron Green's function. This procedure evidently neglects off-shell and finite-lifetime effects. In the same spirit we make the KMK approximation (on-shell approximation for the anomalous Green's function) using the fact that the renormalized problem, with $\lambda^*=\lambda/(\lambda+1)$, is essentially a weak-coupling one. Finally, we propose an approximate two—square-well solution of the renormalized KMK equation. Now, this whole scheme may appear to be far too simple, especially in the light of the fact that so much effort has been invested in recent years to devise computational schemes which can give a reliable $T_c$ in the case of high-frequency attractive mechanisms. Rietschel and Sham[30] have solved the full self-energy equations to calculate the $T_c$ of an electron gas due to plasmon exchange and found that the KMK equation can be in error by orders of magnitude. In our case, however, the situation is not so bad because we are dealing with a *low-frequency* attractive mechanism. The Cooper pairs scatter within an attractive potential well near the Fermi surface. This potential well can be described by its depth (i.e., the static parameters $\lambda$ and $\mu$) and its width (i.e., the characteristic frequency $\omega_0$). It is, in this way, very similar to the original BCS model, and a sensible evaluation of $T_c$ can be given in terms of these three parameters without having to consider the detailed frequency dependence of the interaction. A comparison between various approaches to the calculation of $T_c$ has been carried out for the case of a low-frequency attractive mechanism (i.e., $\lambda>\mu^*$) by Khan and Allen[31] in the limit $\omega_0/E_F\ll 1$. Their results show that McMillan's formula agrees very well with the solution of the Eliashberg equations, whereas the renormalized KMK equation *underestimates* $T_c$. Furthermore, the various $T_c$ differ not by an order of magnitude, but by a factor of 2 or 3 at most. This is, in our opinion, the magnitude of uncertainty which is reasonable to put on our result. A more accurate solution would probably introduce further attraction between the electrons (for example, via plasmon exchange, which cannot be accounted for by the two—square-well solution), and since we have used weak local fields and strong mass renormalization, it is likely that a better calculation will give a higher $T_c$.

From an experimental point of view, the main obstacle to the observation of a superconducting EHL arises from electron-hole recombination. This process is extremely fast in CdS so that an EHL can be only maintained under very intense optical pumping. Even a plasma temperature of 1 K can prove difficult to reach in this case. On the other hand, an EHL in AgBr has a definitely longer lifetime: This system seems, therefore, more suitable for the observation of a superconducting EHL. Another difficulty connected with electron-hole recombination is the fact that the EHL does not grow indefinitely under optical pumping, but rather splits into many droplets of a typical size $\sim 100a_0^*$. In Sec. V we estimated a penetration depth of the order of $10^3a_0^*$. Thus the Meissner effect cannot be observed unless one finds a way of drastically increasing the size of the EHL. This can be achieved by means of a potential-well technique[32] in which many droplets are forced to coalesce within a stress field. Besides the Meissner effect, another manifestation of superconductivity in an EHL would be the appearance of an undamped acoustic plasmon inside the energy gap.[33] This mode would exist for low mass-ratio values, where, in the normal state, it would be substantially broader.

Although we have considered only EHL's in this paper, the model is applicable to an electron-hole system in thermodynamic equilibrium provided that hybridization between electron and hole bands can be neglected. Such a system would be free of recombination effects, and should exhibit the phenomenon of superconductivity if the density, masses, and dielectric constants have favorable values.

## ACKNOWLEDGMENTS

This work was supported in part by the National Science Foundation (NSF) under Grant No. DMR-80-11934 and by the Materials Research Center of Northwestern University under a grant from the NSF.

## APPENDIX A: EFFECTIVE INTERACTION IN AN ELECTRON-HOLE LIQUID

In this Appendix we derive the effective interaction between two electrons in an EHL. Since this interaction must be irreducible in the particle-particle channel, all the Feynman diagrams contributing to it must belong to one of the following three classes: (i) diagrams which are reducible in the direct particle-hole channel (i.e., if we call $p_1,p_2$ the four-momenta of the incoming particles and $p_1-q, p_2+q$ those of the outgoing particles, the channel with particle-hole momentum $q$), (ii) diagrams reducible in the "crossed" particle-hole channel (i.e., the one with particle-hole momentum $p_1-p_2-q$), and (iii) diagrams irreducible in both particle-hole channels as well as in the particle-particle channel. The general expansion of the diagrams belonging to the first class is shown in Fig. 12(a). Here the block $\underline{I}$ is assumed to contain all the diagrams which are irreducible in the direct particle-hole channel. $\underline{\Gamma}^d$ therefore represents the sum of all diagrams of class (i). The labels on the external lines indicate the species of the particles (electrons or holes) and their spin orientation relative to an arbitrary axis: $\bar{i}\equiv(i,\sigma_i)$. We are considering, for the moment, a single electron valley and a single hole valley. Thus both $\underline{I}$ and $\underline{\Gamma}^d$ are $4\times 4$ matrices $(\underline{I})_{i,\sigma_i;j,\sigma_j}$ and $(\underline{\Gamma}^d)_{i,\sigma_i;j,\sigma_j}$. A summation over the intermediate label $\bar{k}$ is implied in Fig. 12(a). In order to solve the diagrammatic equations indicated in Fig. 12(a), we need two essential approximations. First, we assume that $\underline{I}$ (and therefore also $\underline{\Gamma}^d$) does not depend on the momenta of the incoming particles, but only on the momentum transfer $q$. Second, we assume that the intermediate lines in Fig. 12 can be replaced by free-particle Green's functions. With these two approximations the integral over the internal four-momentum can be easily done and gives the Lindhard function per component per spin orientation: $\chi_{0k,\sigma_k}(q)=\chi_{0k}(q)/2$. The equation for $\underline{\Gamma}^d(q)$, ex-

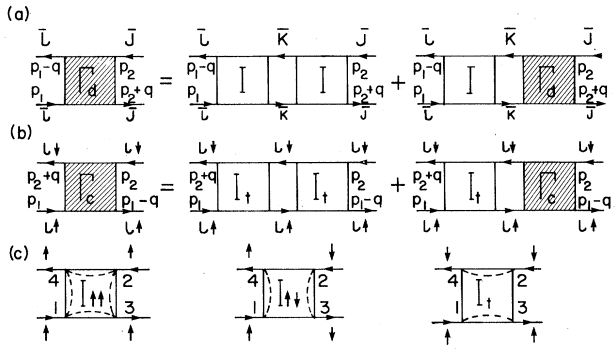

FIG. 12. (a) Diagrammatic representation of the Bethe-Salpeter equation for the interaction reducible in the direct particle-hole channel. (b) Same as (a) for the interaction reducible in the crossed particle-hole channel. (b) Illustration of the relationship between the particle-hole irreducible interactions $I^{\uparrow\uparrow}$, $I^{\uparrow\downarrow}$, and $I^{t}$.

pressed in matrix notation, becomes

$$\underline{\Gamma}^{d}(q)=\underline{I}(q)\underline{\chi}_0(q)\underline{I}(q)+\underline{I}(q)\underline{\chi}_0(q)\underline{\Gamma}^{d}(q)\ , \tag{A1}$$

where

$$(\underline{\chi}_0)_{k,\sigma_k;l,\sigma_l}\equiv\chi_{0k,\sigma_k}\delta_{k,l}\delta_{\sigma_k,\sigma_l}\ ,$$

and the matrix product is understood. This equation can be easily solved to yield

$$\underline{\Gamma}^{d}(q)=\underline{I}(q)\underline{\chi}(q)\underline{I}(q)\ , \tag{A2}$$

where $\underline{\chi}(q)$ is defined via the relation

$$[\underline{\chi}(q)]^{-1}=[\underline{\chi}_0(q)]^{-1}-\underline{I}(q)\ . \tag{A3}$$

The meaning of the matrix $\underline{\chi}(q)$ is easy to understand from Fig. 12. It represents, within our approximations, the sum of all diagrams beginning with a particle-hole fluctuation in the $\sigma_i$ component of the species labeled $i$ and ending with a particle-hole fluctuation in the $\sigma_j$ component of the species labeled $j$. This is the diagrammatic definition of the partial density-density response function giving the density induced in the $\sigma_i$ component of the $i$th species by a potential which couples linearly to the density of the $\sigma_j$ component of the $j$th species.

Equation (A2) involves $4\times4$ matrices. In a nonmagnetic system, however, its spin dependence can be simplified leading to a set of two equations involving $2\times2$ matrices. In order to do this we observe that any matrix entering Eq. (A2)—say, $\underline{I}(q)$-can be regarded as a set of four $2\times2$ matrices in spin space $(\underline{I}_{i,j})^{\sigma_i,\sigma_j}\equiv\underline{I}_{i,\sigma_i;j,\sigma_j}$. If there is isotropy in spin space, each of the $\underline{I}_{ij}$'s has the form ($2\times2$ matrix)

$$\underline{I}_{ij}=\begin{bmatrix} I_{ij}^{\uparrow\uparrow} & I_{ij}^{\uparrow\downarrow} \\ I_{ij}^{\uparrow\downarrow} & I_{ij}^{\uparrow\uparrow} \end{bmatrix}\ , \tag{A4}$$

with only two independent components $I_{ij}^{\uparrow\uparrow}$ and $I_{ij}^{\uparrow\downarrow}$ (because $I_{ij}^{\downarrow\uparrow}=I_{ij}^{\uparrow\downarrow}$ and $I_{ij}^{\downarrow\downarrow}=I_{ij}^{\uparrow\uparrow}$). Such a matrix can be brought to a diagonal form with eigenvalues $I_{ij}^{+}$ and $I_{ij}^{-}$ given by

$$I_{ij}^{\pm}=I_{ij}^{\uparrow\uparrow}\pm I_{ij}^{\uparrow\downarrow}\ . \tag{A5}$$

Returning to Eq. (A2), we see that it can be rewritten as

$$\underline{\Gamma}_{ij}^{d}(q)=\sum_{k,l=1}^{2}\underline{I}_{ik}(q)\underline{\chi}_{kl}(q)\underline{I}_{lj}(q)\ , \tag{A6}$$

where each "term" is a product of three $2\times2$ matrices in spin space. Diagonalizing both sides of Eq. (A6), we find the eigenvalues

$$\Gamma_{ij}^{d,\pm}(q)=\sum_{k,l=1}^{2}I_{ik}^{\pm}(q)\chi_{kl}^{\pm}(q)I_{lj}^{\pm}(q)\ . \tag{A7}$$

Specializing to the case of interaction between two electrons with antiparallel spin, we find

$$\begin{aligned}\Gamma_{ij}^{d,\uparrow\downarrow}(q)&=\tfrac{1}{2}[\Gamma_{ij}^{d,+}(q)-\Gamma_{ij}^{d,-}(q)]\\&=\tfrac{1}{2}\sum_{k,l=1}^{2}[I_{ik}^{+}(q)\chi_{kl}^{+}(q)I_{lj}^{+}(q)\\&\qquad-I_{ik}^{-}(q)\chi_{kl}^{-}(q)I_{lj}^{-}(q)]\ .\end{aligned} \tag{A8}$$

Let us now examine more closely the meaning of the function $\chi_{ij}^{+}(q)$ and $\chi_{ij}^{-}(q)$. From our identification of $\chi_{ij}^{\uparrow\uparrow}(q)$ and $\chi_{ij}^{\uparrow\downarrow}(q)$ as the partial density-density response functions, and from Eq. (A5), it follows that $\chi_{ij}^{+}$ is equal to *one-half* of the $(i,j)$ component of the density-density response matrix introduced in Sec. II. Similarly, $\chi_{ij}^{-}$ is equal to *one-half* of the spin-spin response function of Sec. II. Explicit expressions for $\chi^{\pm}$ in terms of $\chi_0$'s and $I^{\pm}$'s can be easily worked out from Eq. (A3), and we find that they coincide with one-half of the expressions of Eqs. (6) and (7) for $\chi^{s}$ and $\chi^{a}$ only if we make the identifications

$$I_{ij}^{+}(q)=2\psi_{ij}^{s}(q)\ , \tag{A9a}$$

$$I_{ij}^{-}(q)=2\psi_{ij}^{a}(q)\ , \tag{A9b}$$

with $\psi_{ij}^{s,a}$ defined in Eqs. (3) and (8) (with $\nu_i=1$). Using the fact that the spin-antisymmetric polarization field is diagonal, we finally find

$$\Gamma_{ij}^{d,\uparrow\downarrow}(q)=\sum_{k,l=1}^{2}\psi_{ik}^{s}(q)\chi_{kl}^{s}(q)\psi_{lj}^{s}(q)-[\psi_{ii}^{a}(q)]^{2}\chi_{ii}^{a}(q)\delta_{ij}\ . \tag{A10}$$

We now consider the second class of diagrams, those which are reducible in the crossed particle-hole channel. The general expansion for the diagrams of this class is shown in Fig. 12(b). We concentrate on the interaction between electrons with antiparallel spin since this case encompasses both the singlet and the triplet states. Furthermore, it is evident that this class of diagrams only exists if $i=j$. The interaction block $I^{t}$ in Fig. 12(b) differs from that of Fig. 12(a) because the incoming particle-hole pair has a four-momentum $p_1-p_2-q$ and a spin component $S_z=\pm1$ along the $z$ axis. The difference between $I^{\uparrow\uparrow}$, $I^{\uparrow\downarrow}$, and $I^{t}$ is illustrated in Fig. 12(c). Diagrams of $I^{\uparrow\uparrow}$ can be connected in two different ways, either in the "horizontal" channel (1 joins 3, 2 joins 4) or in the "vertical" channel (1 joins 4, 2 joins 3). Diagrams of $I^{\uparrow\downarrow}$ can only be connected

in the vertical channel and diagrams of $I^t$ can only be connected in the horizontal channel. Since the system is spin isotropic there is no difference between corresponding diagrams in $I^{\uparrow\uparrow}$, $I^{\uparrow\downarrow}$, and $I^t$, and we find

$$I^t(p_1,p_2,q)=I^{\uparrow\uparrow}(p_1,p_2,q)-I^{\uparrow\downarrow}(p_1,p_2,q)\ . \tag{A11}$$

This result is exact and does not depend on our approximations. Now introducing those approximations plus the correspondence just derived between $I$'s and $\psi$'s, we can calculate the sum $\Gamma^c$ of the diagrams of class (ii) and find

$$\begin{aligned}\Gamma^{c,\uparrow\downarrow}_{ii}(p_1-p_2-q)&=-[I^-_{ii}(p_1-p_2-q)]^2\chi^-_{ii}(p_1-p_2-q)\\&=-2[\psi^a_{ii}(p_1-p_2-q)]^2\chi^a_{ii}(p_1-p_2-q)\ ,\end{aligned} \tag{A12}$$

where the minus sign arises from the exchange character of this class of diagrams. It is this part of the interaction which is mediated by transverse spin fluctuations (particle-hole pairs in a triplet state with $S_z=\pm1$). For two electrons in a Cooper pair, the initial momenta are $p_1=-p_2=p_0\sim(\mathbf{p}_F,0)$, and the scattering event reduces to a rotation of the line joining the two electrons in momentum space. The magnitudes of the momentum transfers $q$ and $|2\mathbf{p}_F-\mathbf{q}|$ can be expressed in terms of the angle $\theta$ of this rotation as follows,

$$q=2p_F\sin(\theta/2),\quad |2\mathbf{p}_F-\mathbf{q}|=2p_F\cos(\theta/2)\ , \tag{A13}$$

and the effective interaction can be regarded as a function of $\theta$. From the requirement of antisymmetry of the wave function, if the two electrons are in the singlet state this function can be expanded in a series of Legendre polynomials with *even* $l$, while, if they are in a triplet state, it can be expanded in series of Legendre polynomials with *odd* $l$. Using Eq. (A13), it can be proved that, for any function $f$,

$$\begin{aligned}\int_0^\pi |d\cos\theta|\, f(q)P_l(\cos\theta)&\\=(-1)^l\int_0^\pi |d\cos\theta|\, f(|2\mathbf{p}_F-\mathbf{q}|)&\\\times P_l(\cos\theta)\ .&\end{aligned} \tag{A14}$$

Thus the argument $p_1-p_2-q=2p_F-q$ in Eq. (A12) can be replaced by $q$ without any change if the two electrons are in the singlet state or with the change of the sign if they are in a triplet state:

$$\Gamma^{c,\uparrow\downarrow}_{ii}(p_1-p_2-q)\to\begin{cases}\Gamma^{c,\uparrow\downarrow}_{ii}(q) & \text{for singlet,}\\ -\Gamma^{c,\uparrow\downarrow}_{ii}(q) & \text{for triplet}\ .\end{cases} \tag{A15}$$

Finally, we consider the third class of diagrams, those which are irreducible in the particle-hole and particle-particle channels. The simplest diagram of this class is given by the bare interaction line $\phi_{ij}(q)$. More complex diagrams of this class exist in higher orders of perturbation theory and roughly describe a nonlinear coupling between intermediate density or spin fluctuations. We neglect these diagrams here and this is the origin of the linear structure of Eq. (10). Collecting the results and writing them in invariant notation, we find, for two identical particles in a pair,

$$\begin{aligned}[V_{\rm eff}(q)]_{ii}=v(q)+\sum_{k,l=1}^{2}\psi^s_{ik}(q)\chi^s_{kl}(q)\psi^s_{lj}(q)&\\+[\psi^a_{ii}(q)]^2\chi^a_{ii}(q)\boldsymbol{\sigma}_1\cdot\boldsymbol{\sigma}_2\ ,&\end{aligned} \tag{A16}$$

where $\boldsymbol{\sigma}_1\cdot\boldsymbol{\sigma}_2=1$ in the triplet and $-3$ in the singlet. This gives Eq. (10) for $\nu_i=1$. In order to arrive at Eq. (12), we first separate out the purely electronic part of the interaction, i.e., what remains of Eq. (10) after setting $\chi_{02}=0$. The proper electronic vertex appearing in this part of the interaction is obtained as the solution of the equation.

$$\Lambda_1(q)=1-2\tilde{I}^+_{11}(q)\Lambda_1(q)\ , \tag{A17}$$

which is the local version of the Bethe-Salpeter equation for this quantity. $\tilde{I}^+$ is the proper part (in the sense of Nozières) of the irreducible interaction $I^+$. It is related to the latter by the relation

$$\tilde{I}^+(p_1,p_2,q)=I^+(p_1,p_2,q)-v(q)\to-2v(q)G^s(q)\ , \tag{A18}$$

following from the fact that an irreducible diagram other than the bare interaction line is always proper. This proves Eq. (12a). The expression for $\epsilon_1$ in terms of $\Lambda_1$ also follows from the general definition of the dielectric constant using the local approximation. The detailed derivation of Eq. (12) is only a matter of straightforward algebra and is not given here.

The above derivation of the effective interaction can be easily extended to the case of several equivalent electron and hole valleys. Rather than working out the general form of the interaction, we introduce at the outset the approximation of neglecting intervalley scattering. This approximation enables us to express the effective interaction in terms of only two independent local-field corrections, $G^s$ and $G^a$. Indeed, the problem becomes equivalent to finding the effective interaction in a system of hypothetical electrons and holes having spin $\nu_i-\frac{1}{2}$. Thus, the derivation goes through as in the nondegenerate case with a few obvious changes to take into account the value of the pseudospin. In particular, the matrices $\underline{I}_{ij}$ in Eq. (A4) become $2\nu_i\times2\nu_j$ matrices. The square matrices $\underline{I}_{ii}$ can be brought to a diagonal form with eigenvalues

$$I^+_{ii}=I^{\uparrow\uparrow}_{ii}+(2\nu_i-1)I^{\uparrow\downarrow}_{ii},\quad I^-_{ii}=I^{\uparrow\uparrow}_{ii}-I^{\uparrow\downarrow}_{ii}\ , \tag{A19}$$

and the possibly rectangular matrices $\underline{I}_{ij}$ are brought, by the same transformation, to a form with a single nonvanishing element in the upper left corner:

$$I^+_{ij}=(\nu_i\nu_j)^{1/2}I_{ij},\quad i\neq j \tag{A20}$$

($I^-_{ij}=0$ as before). The $\chi^\pm_{ij}$ correspond to the density-density ($+$) and spin-spin ($-$) response functions divided by $2(\nu_i\nu_j)^{1/2}$. This leads to the identification

$$I^+_{ij}(q)=2(\nu_i\nu_j)^{1/2}\psi^s_{ij}(q),\quad I^-_{ij}(q)=2(\nu_i\nu_j)^{1/2}\psi^a_{ij}(q)\ , \tag{A21}$$

which generalizes Eqs. (A9). Inserting these results into

Eq. (A8), we easily verify that Eq. (A10) remains valid. Similarly, Eqs. (A11) and the first of Eqs. (A12) remain valid, which gives

$$\Gamma^c_{ii}(p_1-p_2-q)=-2\nu_i[\psi^a_{ii}(p_1-p_2-q)]^2\chi^a_{ii}(p_1-p_2-q)\ , \tag{A22}$$

proving the presence of the degeneracy factor $\nu_i$ in front of the transverse spin-fluctuation term. Transforming the argument $p_1-p_2-q$ to $q$ for the singlet interaction, and adding the totally irreducible term $v(q)$ plus the other term $\Gamma^c(q)$, we arrive at the result of Eq. (10).

## APPENDIX B: CONDITIONS OF STABILITY FOR AN ELECTRON-HOLE LIQUID

In this Appendix we discuss the important question of whether spin-density or charge-density waves (SDW's and CDW's) can occur in an EHL before the superconducting transition and suppress it. It is well known from general considerations and from detailed calculations that strong Coulomb correlations in the electron liquid act to inhibit spin instabilities. In the electron gas, for example, a transition to the ferromagnetic state is expected[34] only at a very large value of the coupling constant, $r_s\sim 70$. In the EHL the effective coupling constant for each component is $r_s m_i/\mu$. Even at a mass ratio 10, a ferromagnetic instability of the holes would occur at $r_s\sim 7$, which is well beyond the range of attainable $r_s$. It seems, therefore, very likely that if any instability other than the superconducting one is going to occur in an EHL, it is going to be a CDW. In the case of a simple metal it has been shown[35] that both exchange and correlation favor this instability, while the main opposing force is the rigidity of the ionic background. There is no such background in the EHL, the holes themselves being a highly mobile plasma. Thus it seems that we have found a very good candidate for a CDW instability. The presence of a CDW is not, however, incompatible with superconductivity. Its main effect on the electrons is to add a self-consistent periodic potential that does not interfere with the pairing in time-reversed states. The electronic density of states is changed near the Fermi surface by an amount proportional to $G/E_F$, where $G$ is the amplitude of the self-consistent potential. This is presumably a very small correction. There is, however, one important point that must be checked. If CDW's (or, for that matter, SDW's) occurred as continuous transitions at a certain critical density (i.e., with infinitesimal amplitude), a zero-frequency collective mode would appear that would make our interaction singular in the low-frequency limit. This singularity is unphysical and simply means that the homogeneous paramagnetic ground state which we assumed in constructing the interaction is no longer a good starting point. It is important, therefore, to be sure that we are not using our effective interaction beyond a second-order transition point. Here we give the conditions that ensure the stability of the ground state against such continuous transitions. Let us consider CDW's first. At $T=0$ the energy of an EHL with an infinitesimal CDW in it is given by the Hohenberg-Kohn expansion of Eq. (16), where the $\delta n_i$ are the amplitudes of the CDW and the summation over $q$ is restricted to the wave vector of the CDW. The CDW will not occur spontaneously if the energy of this state is higher than the energy of the homogeneous ground state. Thus, the condition for stability against infinitesimal CDW's of wave vector $Q$ is that the response matrix $\chi^s(Q)$ be *negative* definite (i.e., that all its eigenvalues be negative). Using the GRPA expression for $\chi$, we find that this condition corresponds to the set of inequalities

$$[1-\psi_{11}\chi_{01}(Q,0)][1-\psi_{22}\chi_{02}(Q,0)] -\psi^2_{12}(Q)\chi_{01}(Q,0)\chi_{02}(Q,0)>0 \tag{B1}$$

and

$$\chi_{01}(Q,0)+\chi_{02}(Q,0) -[\psi_{11}(Q)+\psi_{22}(Q)]\chi_{01}(q,0)\chi_{02}(Q,0)<0\ .$$

Similarly, the condition of stability against infinitesimal SDW's of wave vector $Q$ is $\chi^a_{ii}(Q,0)<0$ for $i=1,2$, or, explicitly,

$$1-\psi_{ii}(Q)\chi_{0i}(Q,0)>0,\quad i=1,2\ . \tag{B2}$$

In the limit of small $Q$, Eqs. (B1) and (B2) reduce to the requirement that the compressibility and spin susceptibility of the system be positive and finite. These conditions are always satisfied in our calculation. The problem now arises whether inequalities (B1) and (B2) can be violated at finite $Q$ while being satisfied for $Q\to 0$. Since $v(q)$ and $\chi_0(q,0)$ are both rapidly decreasing functions of $q$, this possibility is unlikely, unless the local-field factors increase very rapidly in the small-$q$ region. Such a behavior could arise if, for example, the local-field factors had a strong peak at intermediate wave vector. Our parameterized local fields, however, do not have any peak, and inequalities (B1) and (B2) are satisfied, in our model, for all values of $Q$. The effective interaction remains regular throughout the range of our calculations.

## APPENDIX C: APPROXIMATE FORMULA FOR THE CRITICAL TEMPERATURE

In this Appendix we give some details on the derivation of the approximate formula for $T_c$ [Eq. (52a)]. The KMK equation is

$$\phi(p)=-\sum_{\mathbf{k}}\frac{1}{2\epsilon_{\mathbf{k}}}K(\mathbf{p},\mathbf{k})\tanh\left[\frac{\epsilon_k}{2T_c}\right]\phi(k)\ , \tag{C1}$$

where

$$K(\mathbf{p},\mathbf{k})=U_c(\mathbf{p}-\mathbf{k})+\frac{2}{\pi}\int_0^\infty d\epsilon\frac{\mathrm{Im}U_h(\mathbf{p}-\mathbf{k},\epsilon)}{\epsilon+|\epsilon_p|+|\epsilon_k|}\ . \tag{C2}$$

The electronic interaction $U_c$ is approximated by its static limit. $\epsilon_p$ and $\epsilon_k$ are free-electron energies measured with respect to the chemical potential.

The modified KMK equation is derived in exactly the same way as the original one, using, instead of the free-particle Green's function, the modified Green's function of Eq. (54). The KMK ansatz [Eq. (53)] is also expressed in terms of the renormalized energies $\epsilon^*_p=\epsilon_p Z^{-1}$

$=\epsilon_p m/m^*$. As a result of these modifications, the kernel of Eq. (C2) is simply multiplied by a factor $Z^{-2}$, and all the free-electron energies in Eqs. (C1) and (C2) are replaced by renormalized energies. It is convenient to express the magnitude of the vectors $\mathbf{p}$ and $\mathbf{k}$ in terms of the corresponding free-electron energies, i.e., we introduce

$$\omega=\epsilon_p^*,\quad \omega'=\epsilon_k^*,\quad k\,dk=m^*\,d\omega'=mZ\,d\omega\ . \tag{C3}$$

The modified equation (C1) becomes

$$\phi(\omega)=-\int_{-E_{F1}}^{+\infty}d\omega'\,\phi(\omega')\frac{1}{2\omega'}\tanh\left[\frac{\omega'}{2T_c}\right]\left[\frac{Z^{-1}m}{4\pi^2 p(\omega)}\int_{|p(\omega)-p(\omega')|}^{|p(\omega)+p(\omega')|}dq\,qK(\omega,\omega';q)\right], \tag{C4}$$

where

$$p(\omega)=[2m^*(\omega+E_{F1})]^{1/2}\ , \tag{C5}$$

and we have set $K(\mathbf{p},\mathbf{k})=K(|\mathbf{p}|,|\mathbf{k}|;|\mathbf{p}-\mathbf{k}|)$. In Eq. (C4) we set $p(\omega)\cong p(\omega')=p(0)\cong q_F$. This approximation is justified for the dynamic part of the kernel since the characteristic frequency is a small fraction of $E_{F1}$, and it is also reasonable for the Coulomb part of the kernel because this quantity depends very slightly on $\omega$ and $\omega'$.

Using Eq. (C2) in Eq. (C4), together with Eq. (12) and the definitions of $\mu$ and $\alpha^2F(\omega)$ [Eqs. (46) and (48)], we rewrite Eq. (C4) as

$$\phi(\omega)=-\mu Z^{-1}\int_{-E_{F1}}^{+\infty}d\omega'\,\phi(\omega')\frac{1}{2\omega'}\tanh\left[\frac{\omega'}{2T_c}\right]+Z^{-1}\int_{-E_{F1}}^{+\infty}d\omega'\,\phi(\omega')\frac{1}{2\omega'}\tanh\left[\frac{\omega'}{2T_c}\right]$$
$$\times\int_0^\infty\alpha^2F(\epsilon)\frac{2}{\epsilon+|\omega|+|\omega'|}d\epsilon\ . \tag{C6}$$

We put an upper cutoff $E_{F1}$ for the $\omega'$ integral and define the trial function

$$\phi(\omega)=\begin{cases}\phi_0, & |\omega|<\omega_0\\ \phi_\infty, & |\omega|>\omega_0\end{cases} \tag{C7}$$

where $\omega_0$ is the characteristic frequency of Eq. (47). Evaluating Eq. (C6) at zero frequency, we find

$$\phi(0)=\phi_0\cong Z^{-1}\left[\phi_0\int_0^{\omega_0}d\omega'\frac{1}{\omega'}\tanh\left[\frac{\omega'}{2T_c}\right]\int_0^\infty\alpha^2F(\epsilon)\frac{2}{\epsilon}d\epsilon+\phi_\infty\int_{\omega_0}^{E_{F1}}\frac{d\omega'}{\omega'}\int_0^\infty\alpha^2F(\epsilon)\frac{2}{\epsilon+|\omega'|}d\epsilon\right]$$
$$-\mu Z^{-1}\left[\phi_0\int_0^{\omega_0}d\omega'\frac{1}{\omega'}\tanh\left[\frac{\omega'}{2T_c}\right]+\phi_\infty\int_{\omega_0}^{E_{F1}}\frac{d\omega'}{\omega'}\right], \tag{C8}$$

where we set $\tanh(\omega'/2T_c)\sim 1$ in the high-frequency integrals ($\omega'>\omega_0$) and neglect $\omega'$ with respect to $\epsilon$ in the first integral.

The integrals over $\omega'$ can be evaluated analytically and we find

$$\phi_0=Z^{-1}\left\{\phi_0\ln\left[\frac{2\gamma\omega_0}{\pi T_c}\right](\lambda-\mu)\right.$$
$$\left.+\phi_\infty\left[Q-\mu\ln\left[\frac{E_F}{\omega_0}\right]\right]\right\}, \tag{C9}$$

where $\lambda$ is defined in Eq. (49), and

$$Q\cong\int_0^\infty d\epsilon\,\alpha^2F(\epsilon)\frac{2}{\epsilon}\ln\left[1+\frac{\epsilon}{\omega_0}\right]. \tag{C10}$$

Here, $\gamma=e^c$, where $c$ is the Euler constant, $2\gamma/\pi\cong 1.14$. Evaluating (C6) at a frequency large compared to $\omega_0$, we can drop the dynamic part of the kernel as well as the mass renormalization $Z$, and we find

$$\phi_\infty\cong-\mu\ln\left[\frac{2\gamma\omega_0}{\pi T_c}\right]\phi_0-\mu\ln\left[\frac{E_{F1}}{\omega_0}\right]\phi_\infty\ . \tag{C11}$$

Equations (C11) and (C9) form a set of homogeneous equations which has a nontrivial solution only if

$$T_c\cong 1.14\omega_0\exp\left[-\frac{Z}{\lambda-\mu^*(1+Q)}\right]. \tag{C12}$$

In order to estimate $Q$, let us take the simple model

$$\alpha^2F(\omega)=\lambda\frac{\omega}{\omega_m}\left[1-\frac{\omega}{\omega_m}\right]\Theta(\omega_m-\omega)\ , \tag{C13}$$

in which the spectrum vanishes for $\omega>\omega_m$. The characteristic frequency in this model is

$$\omega_0=\omega_m e^{-3/2}\ , \tag{C14}$$

which, for $\omega_0\sim E_{Fh}$, gives the reasonable cutoff $\omega_m\sim 4.5E_{Fh}$. Evaluating $Q$ for this model, we find

$$Q=0.822\lambda\ . \tag{C15}$$

Notice that McMillan's formula gives $Q\cong 0.64\lambda$. We underestimate the critical temperature if we take $Q\cong\lambda$. This gives Eq. (52a).

*Present address: Max-Planck-Institut für Festkörperforschung, 7000 Stuttgart 80, Federal Republic of Germany.

[1]T. M. Rice, in *Solid State Physics,* edited by H. Ehrenreich, F. Seitz, and D. Turnbull (Academic, New York, 1977), Vol. 32, p. 1; P. Vashishta, R. K. Kalia, and K. S. Singwi, in *Electron-Hole Droplets in Semiconductors,* edited by L. V. Keldysh and C. D. Jeffries (North-Holland, Amsterdam, 1983).

[2]D. Pines, Can. J. Phys. **34**, 1379 (1956).

[3]G. Vignale and K. S. Singwi, Solid State Commun. **44**, 259 (1982).

[4]J. W. Garland, in *Proceedings of the Eighth International Conference on Low-Temperature Physics,* edited by R. O. Davies (Butterworths, Boston, Mass. 1963), p. 143.

[5]M. L. Cohen and P. W. Anderson, in *Superconductivity in d- and f-band Metals,* edited by D. H. Douglass (AIP, New York, 1972), p. 17.

[6]K. S. Singwi, M. P. Tosi, R. H. Land, and A. Sjölander, Phys. Rev. **176**, 589 (1968).

[7]P. Vashishta, P. Bhattacharyya, and K. S. Singwi, Phys. Rev. B **10**, 5108 (1974).

[8]C. A. Kukkonen and A. W. Overhauser, Phys. Rev. B **20**, 550 (1979).

[9]R. F. Leheny and Jagdeeph Shah, Phys. Rev. Lett. **37**, 871 (1976); **38**, 511 (1977).

[10]D. Hulin, A. Mysyrowicz, M. Combescot, I. Pelant, and C. Benoît à la Guillaume, Phys. Rev. Lett. **39**, 1169 (1977).

[11]V. Heine, P. Nozières, and J. W. Wilkins, Philos. Mag. **13**, 741 (1965).

[12]J. E. Jaffe and N. W. Ashcroft, Phys. Rev. B **23**, 6176 (1981).

[13]J. M. Whitmore, J. P. Carbotte, and R. C. Shukla, Can. J. Phys. **57**, 1185 (1979).

[14]G. Vignale and K. S. Singwi (unpublished).

[15]C. A. Kukkonen and J. W. Wilkins, Phys. Rev. B **20**, 550 (1979).

[16]P. Nozières, *Theory of Interacting Fermi Systems* (Benjamin, New York, 1964), p. 287.

[17]Naoki Iwamoto and D. Pines, Phys. Rev. B **29**, 3924 (1984).

[18]P. Hohenberg and W. Kohn, Phys. Rev. **136**, B864 (1964).

[19]Tapash Chakraborty and P. Pietiläinen, Phys. Rev. Lett. **49**, 1034 (1982).

[20]J. C. Culberston and J. E. Furneaux, Phys. Rev. Lett. **49**, 1528 (1982).

[21]G. Gladstone, M. A. Jensen, and J. R. Schrieffer, in *Superconductivity,* edited by R. D. Parks (Dekker, New York, 1969), p. 729.

[22]C. A. Kukkonen and H. Smith, Phys. Rev. B **8**, 4601 (1973).

[23]*High Temperature Superconductivity,* edited by V. L. Ginzburg and D. A. Kirzhnits (Consultants Bureau, New York, 1982), p. 77.

[24]W. L. McMillan, Phys. Rev. **167**, 331 (1968).

[25]D. A. Kirzhnits, E. G. Maksimov, and D. I. Khomskii, J. Low. Temp. Phys. **10**, 79 (1973).

[26]G. Beni and T. M. Rice, Phys. Rev. B **18**, 768 (1978).

[27]E. A. Pashitskii and V. M. Chernousenko, Zh. Eksp. Teor. Fiz. **60**, 1483 (1971) [Sov. Phys.—JETP **33**, 802 (1971)].

[28]P. Bhattacharyya and Sudanshu S. Jha, J. Phys. C **11**, L805 (1978).

[29]A. Holas, P. K. Aravind, and K. S. Singwi, Phys. Rev. B **20**, 4912 (1979); **25**, 561 (1981).

[30]H. Rietschel and L. J. Sham, Phys. Rev. B **28**, 5100 (1983).

[31]F. S. Kahn and P. B. Allen, Solid State Commun. **36**, 481 (1980).

[32]P. L. Gourley and J. Wolfe, Phys. Rev. B **24**, 5970 (1981).

[33]G. Vignale and K. S. Singwi (unpublished).

[34]H. Ceperley and C. A. Alder, Phys. Rev. Lett. **45**, 566 (1980).

[35]A. W. Overhauser, Adv. Phys. **27**, 343 (1978).